bioRxiv preprint doi: https://doi.org/10.1101/2023.04.11.536332; this version posted April 12, 2023. The copyright holder for this preprint (which was not certified by peer review) is the author/funder, who has granted bioRxiv a license to display the preprint in perpetuity. It is made available under aCC-BY 4.0 International license.

Oligodendrocyte-derived IL-33 functions as a microglial survival factor during neuroinvasive flavivirus infection

Geoffrey T. Norris[1], Joshua M. Ames[1], Steven F. Ziegler[1,2], Andrew Oberst[1,3,*]

[1]Department of Immunology, University of Washington, Seattle WA 98109, USA

[2]Immunology Program, Benaroya Research Institute, Seattle WA 98101, USA

[3]Lead Contact

[*]Correspondence: Oberst@UW.edu

bioRxiv preprint doi: https://doi.org/10.1101/2023.04.11.536332; this version posted April 12, 2023. The copyright holder for this preprint (which was not certified by peer review) is the author/funder, who has granted bioRxiv a license to display the preprint in perpetuity. It is made available under aCC-BY 4.0 International license.

Abstract

In order to recover from infection, organisms must balance robust immune responses to pathogens with the tolerance of immune-mediated pathology. This balance is particularly critical within the central nervous system, whose complex architecture, essential function, and limited capacity for self-renewal render it susceptible to both pathogen- and immune-mediated pathology. Here, we identify the alarmin IL-33 and its receptor ST2 as critical for host survival to neuroinvasive flavivirus infection. We identify oligodendrocytes as the critical source of IL-33, and microglia as the key cellular responders. Notably, we find that the IL-33/ST2 axis does not impact viral control or adaptive immune responses; rather, it is required to promote the activation and survival of microglia. In the absence of intact IL-33/ST2 signaling in the brain, neuroinvasive flavivirus infection triggered aberrant recruitment of monocyte-derived peripheral immune cells, increased neuronal stress, and neuronal cell death, effects that compromised organismal survival. These findings identify IL-33 as a critical mediator of CNS tolerance to pathogen-initiated immunity and inflammation.

KEYWORDS: West Nile virus, Zika virus, inflammation, neuroinflammation, microglia, disease tolerance,

Author Summary

The central nervous system (CNS) is an extraordinarily complex organ system with limited capacity for repair and renewal. When infectious pathogens invade the CNS, resulting immune responses must clear the pathogen while limiting immune-mediated

bioRxiv preprint doi: https://doi.org/10.1101/2023.04.11.536332; this version posted April 12, 2023. The copyright holder for this preprint (which was not certified by peer review) is the author/funder, who has granted bioRxiv a license to display the preprint in perpetuity. It is made available under aCC-BY 4.0 International license.

tissue pathology. IL-33 is an “alarmin” cytokine, whose release from dying cells can promote a variety of immune responses. IL-33 is expressed at high levels in the brain, and previous work has implicated signaling by IL-33 in CNS development as well as in the response to parasitic infection of the CNS. Here, we identify IL-33 as a key mediator of disease tolerance in the context of neuroinvasive infection with the flaviviruses West Nile virus and Zika virus. Notably, we find that IL-33 signaling is not involved in the clearance of virus from the brain; rather, IL-33 is required to promote the survival and reprogramming brain-resident immune cells (microglia). When IL-33 signaling is disrupted in mice, flavivirus infection results in defective microglial activation, increased death of both microglia and neurons, increased invasion of the brain by peripheral immune cells, and increased host death. This work suggests that IL-33 is a key mediator of host tolerance upon neuroinvasive flavivirus infection.

Introduction

Immune responses within the central nervous system (CNS) must both clear pathogens and avoid immune-mediated damage to the complex neuronal architecture that makes up this organ system. As the resident cells immune cells of the CNS, microglia are ideally positioned to mediate both pathogen elimination and tissue preservation. Microglia are long-lived tissue resident macrophages unique in their origin entirely from embryonic yolk sac progenitors with no contribution from other hematopoietic compartments, barring significant CNS disease[1]. Recent advances have described multiple roles for microglia in both CNS homeostasis and upon its perturbation [2,3]. Recent studies have also revealed

bioRxiv preprint doi: https://doi.org/10.1101/2023.04.11.536332; this version posted April 12, 2023. The copyright holder for this preprint (which was not certified by peer review) is the author/funder, who has granted bioRxiv a license to display the preprint in perpetuity. It is made available under aCC-BY 4.0 International license.

mechanisms of microglial function during CNS viral infection [4], where microglia have been shown to contain infection and tissue damage during acute infection, while mediating neuronal and tissue damage if aberrantly activated during recovery. These findings highlight the pleotropic nature of microglial functions in the CNS, and point to a need to better understand the signals that promote the distinct roles of this cell type.

The cytokine IL-33 is a member of the IL-1 family of alarmin cytokines. IL-33 is normally released by damaged or necrotic cells, signaling in a paracrine manner to bystanders expressing the IL-33 receptor ST2 (encoded by *Il1rl1).* IL-33/ST2 signaling has divergent roles in peripheral immune responses, notably contributing to both immune cell activation and tissue homeostasis, including roles in promoting macrophage survival [5]. Notably, IL-33 is highly expressed the CNS, and several roles for IL-33 in CNS development and pathology have been identified, including promotion of synaptic pruning and extracellular matrix remodeling by microglia [6,7], and promotion of recovery from spinal cord injury through macrophage signaling [8]. IL-33 signaling from astrocytes to microglia has also been identified as a driver of protective immune responses to *Toxoplasma gondii* in the brain [9]. However, while the related alarmin IL-1 has been implicated in promoting sequalae to flavivirus infection [10], whether IL-33 contributes to beneficial or pathogenic responses to neurotropic viral infection remains unexplored.

Since its arrival in the Western Hemisphere, the flavivirus West Nile virus (WNV) has become a significant threat to public health, with the majority of disease burden resulting from neuroinvasive infection [11–13]. Recent studies using an attenuated strain of West Nile virus, termed WNV-E218A, as well as a less neurovirulent form of the related Zika virus (ZIKV-Dakar), have shown bivalent roles for resident microglia in promoting

bioRxiv preprint doi: https://doi.org/10.1101/2023.04.11.536332; this version posted April 12, 2023. The copyright holder for this preprint (which was not certified by peer review) is the author/funder, who has granted bioRxiv a license to display the preprint in perpetuity. It is made available under aCC-BY 4.0 International license.

neurological pathology and cognitive sequelae to flavivirus infection, while also contributing to host survival during acute infection. [10,14–16]. Specifically, during acute infection microglia were shown to phagocytose neuronal processes the murine hippocampus, a phenomenon that limits viral dissemination while causing disease sequelae specific to episodic spatial memory [17]. However, pharmacological removal of microglia yielded decreased host and neuronal survival, with minimal changes in viral titer [16], suggesting that microglia play essential roles in host survival during neuroinvasive viral infection.

In this study, we show that IL-33 signaling promotes survival during flavivirus infection, an effect apparently independent of a role for IL-33 in viral control. We found that following CNS infection oligodendrocyte numbers acutely decrease, with IL-33 expression by oligodendrocytes necessary for host survival, implicating release of IL-33 from dying oligodendrocytes. The target of IL-33 signaling was primarily microglia, as mice with specific deletion of ST2 on microglia succumbed more readily to CNS disease. In these mice, we found defects in microglial activation and survival, leading to enhanced BBB breakdown, increased monocyte extravasation and neuronal apoptosis. Together, our studies reveal a source for CNS IL-33 during flavivirus infection and highlight its role in promoting microglial fitness in this setting. These findings suggest that IL-33 signaling is required for CNS tolerance to the inflammatory response triggered by neuroinvasive flavivirus infection.

Results

IL-33/ST2 signaling promotes survival upon neuroinvasive flavivirus infection

bioRxiv preprint doi: https://doi.org/10.1101/2023.04.11.536332; this version posted April 12, 2023. The copyright holder for this preprint (which was not certified by peer review) is the author/funder, who has granted bioRxiv a license to display the preprint in perpetuity. It is made available under aCC-BY 4.0 International license.

We sought to assess the role of IL-33 and its receptor ST2 in controlling the CNS pathogenesis of flavivirus infection. In order to isolate roles for IL-33 and ST2 within the CNS, we used an established model of intracranial infection with an attenuated form of WNV (WNV-E218A), a model in which most wild-type mice survive infection but display CNS pathology and sequelae [14,18] **(Fig S1A)**. To study the role of the IL-33/ST2 pathway in these infection models, we infected *Il1rl1*$^{-/-}$, *Il33*$^{-/-}$, and wild type congenic animals with WNV-E218, then monitored their survival. While ~75% of wild type animals survived infection, both *Il1rl1*$^{-/-}$ and *Il33*$^{-/-}$ mice were significantly more susceptible to WNV-E218A infection, displaying reduced survival and enhanced weight loss **(Figs 1A and S1B)**. We reasoned that this increase in susceptibility could be due to a failure to control viral replication within the CNS. To test this, we titered virus from the cortex, hippocampus, cerebellum, brainstem, and peripheral organs of *Il1rl1*$^{-/-}$, *Il33*$^{-/-}$, and B6/J infected mice at 7 days post-infection (DPI), a timepoint that corresponds to peak disease [14]. While no virus was detected in the periphery of these animals, only the cortex exhibited varying degrees of infectious virus titer **(Fig 1B)**. Surprisingly, *Il33*$^{-/-}$ animals displayed lower levels of viral titers compared to controls while *Il1rl1*$^{-/-}$ titers were higher than WT. No differences in viral titer were seen in other CNS regions.

Since WNV-E218A is an attenuated flavivirus sensitive to the interferon stimulated gene IFIT1 [19], we tested the effects of IL-33 and ST2 deletion with a wild-type isolate of the related flavivirus Zika virus, termed ZIKV-Dakar. While intracranial infection of congenic WT animals yielded ~90% survival, *Il1rl1*$^{-/-}$ mice were significantly more susceptible to infection with survivorship at ~70%. *Il33*$^{-/-}$ mice had a further decrease in survivorship at ~30% with both genotypes showing increased weight loss **(Figs 1C and**

bioRxiv preprint doi: https://doi.org/10.1101/2023.04.11.536332; this version posted April 12, 2023. The copyright holder for this preprint (which was not certified by peer review) is the author/funder, who has granted bioRxiv a license to display the preprint in perpetuity. It is made available under aCC-BY 4.0 International license.

S1C). Upon examination of viral titers from the tissues of these animals we observed that, similarly to WNV-E218A infection, no virus was detected in peripheral tissues **(Fig. 1D)**. Within the CNS only the brainstem showed differences in viral titer upon loss of IL-33/ST2 signaling upon ZIKV-Dakar infection, with *Il1rl1*$^{-/-}$ mice showing lower levels of infectious virus than either WT or *Il33*$^{-/-}$ animals **(Fig. 1D)**. We also assessed the role of IL-33/ST2 signaling in models of peripheral flavivirus infection, and observed increased mortality and weight loss in *Il1rl1*$^{-/-}$ mice (**Figs S1D and S1E**). Further, titering infected tissues of these mice showed no statistically significant differences in CNS or peripheral organ viral titer **(Fig S1F).** Collectively these results suggest that the IL-33/ST2 signaling pathway is important for host survival upon neuroinvasive WNV infection, but that this activity is independent of a role in controlling viral replication or dissemination.

Oligodendrocyte-derived IL-33 promotes survival upon neuroinvasive WNV infection

Since our studies of knockout mice suggested a role for IL-33 in promoting survival to neuroinvasive flavivirus infection, we next sought to assess the source of IL-33 in this setting. We first analyzed the expression and localization of IL-33 in the uninfected CNS and found that IL-33 was exclusively expressed in either oligodendrocytes (Olig2+) or astrocytes (GFAP+) in concordance with prior studies [8,9] **(Fig 2A).** Since IL-33 signaling is associated with its release from dying cells, the loss of IL-33^{+} cells has been used as a surrogate for IL-33 activity [8,9]. To examine the release of IL-33 by Olig2 or GFAP-expressing cells, we intracranially infected C57Bl6/J mice with WNV-E218A and sacrificed animals during peak CNS disease at 7 DPI, preserving their brains for IHC

bioRxiv preprint doi: https://doi.org/10.1101/2023.04.11.536332; this version posted April 12, 2023. The copyright holder for this preprint (which was not certified by peer review) is the author/funder, who has granted bioRxiv a license to display the preprint in perpetuity. It is made available under aCC-BY 4.0 International license.

analysis. Examining hippocampal sub regions of CA3, an area known for synaptic stripping and inflammation during CNS infection, we observed a loss of both IL-33+ astrocytes and IL-33+ oligodendrocytes 7 days post-infection (**Figs 2B and 2C**).

Since IL-33 release is classically associated with cell death we next quantified the number of both astrocytes and oligodendrocytes post-infection. While total GFAP+ astrocyte numbers were stable (**Fig S2A**), Olig2+ oligodendrocyte cell numbers were decreased not only in CA3 sub regions but across the CNS post-infection **(Figs 2D and 2E)**. Given the loss of Olig2+IL-33+ cells in regions of known synaptic stripping and the observation that oligodendrocyte numbers decrease across the CNS during infection, as well as previous studies that have shown oligodendrocyte cell death upon flavivirus infection *in vitro* and *in vivo*[20–22], we hypothesized that oligodendrocytes represented a probable source of released IL-33 following neuroinvasive WNV infection. To test this, we crossed *Plp1*$^{ERT2Cre/+}$ mice with *Il33*$^{fl/fl}$ animals to generate mice lacking IL-33 in oligodendrocytes. We first confirmed that tamoxifen treatment induced the excision of IL-33 from Olig2+ cells without impacting total Olig2+ cell number **(Figs S2B-S2C)**. We next intracranially infected tamoxifen-treated *Plp1*$^{ERT2Cre/+}$::*Il33*$^{fl/fl}$ mice, as well as Cre-negative littermates, with WNV-E218A. Strikingly, Cre+ animals exhibited a survival phenotype closely matching that of global IL-33 deficient animals **(Fig 2F)**. Collectively, these data indicate that oligodendrocyte loss is widespread following CNS WNV infection, and that oligodendrocyte-derived IL-33 promotes host survival.

The IL-33/ST2 signaling axis promotes survival independent of adaptive immunity during neuroinvasive flavivirus infection

bioRxiv preprint doi: https://doi.org/10.1101/2023.04.11.536332; this version posted April 12, 2023. The copyright holder for this preprint (which was not certified by peer review) is the author/funder, who has granted bioRxiv a license to display the preprint in perpetuity. It is made available under aCC-BY 4.0 International license.

186 The IL-33/ST2 signaling pathway has well-defined roles in T cell activation during
187 viral infection, with CD8+ [23], CD4+ [24], and Treg cells [25] implicated. Notably, these three
188 adaptive immune cell types are all critical for WNV host defense [26,27]. We therefore
189 wondered if the survival defect observed in *Il33*$^{-/-}$ or *Il1rl1*$^{-/-}$ mice upon neuroinvasive
190 flavivirus infection was due to altered T cell recruitment or activation. To examine this, we
191 infected both WT and *Il33*$^{-/-}$ mice intracranially with WNV-E218A or ZIKV-Dakar and
192 sacrificed each at 7 days post-infection, removing and processing the brain parenchyma
193 for examination of T cell responses by flow cytometry. Remarkably, there was no change
194 in the number of adaptive effector cells in response to WNV-E218A in *Il33*$^{-/-}$ animals **(Fig**
195 **3A)**. While there was a modest increase in overall T cell number with ZIKV-Dakar
196 infection in *Il33*$^{-/-}$ mice, no differences in Tconv, Treg, or CD8 T cells were seen in *Il33*$^{-/-}$
197 animals with ZIKV-Dakar infection, with MFIs of CD44 and CD69 unchanged in Tconv
198 and CD8 T cells **(Fig 3B)**. Despite these data, and given the essential role of CD8 T cells
199 in CNS protection during WT WNV infection [28], we sought to functionally test their role by
200 depleting CD8 T cells from WT animals and infecting both control and CD8 T cell-depleted
201 mice with WNV-E218A to monitor survival **(Fig S3A)**. Despite robust CD8 T cell depletion,
202 especially among NS4b+ CD8 T cells specific to WNV **(Fig S3B),** no change in survival
203 or weight loss was observed (**Figs S3C and S3D**).

204 To further assess a role for IL-33/ST2 signaling in adaptive immunity, we sought
205 to define which leukocyte subsets express ST2 during infection. To do this, we analyzed
206 both mock and WNV-E218A infected WT mice by flow cytometry at 7 DPI to investigate
207 ST2 expression on CNS immune cells (**Fig S3E**)**.** While HBSS-injected animals showed
208 highest ST2 expression on CD8+ and CD4+ T cells (**Fig 3C**), during infection we observed

bioRxiv preprint doi: https://doi.org/10.1101/2023.04.11.536332; this version posted April 12, 2023. The copyright holder for this preprint (which was not certified by peer review) is the author/funder, who has granted bioRxiv a license to display the preprint in perpetuity. It is made available under aCC-BY 4.0 International license.

the highest proportion of ST2+ cells among Tregs (~8%), followed by Tconv (~2%), and CD45+Non-LymphoidCD11b- cells (~1%); the latter likely representing meningeal innate lymphoid type 2 cells (ILC2s) which are known to express ST2 [29] and exhibited the highest levels of ST2 by MFI **(Figs 3D and S3F)**. As Tregs are known to be critical for host survival following WNV infection and exhibited the highest proportion of ST2 positivity by any of the examined leukocytes **(Figs 3D and S3F)** we tested whether lack of IL-33/ST2 signaling on Treg cells contributed to the observed survival defects following neuroinvasive flavivirus infection. To assess this, we crossed *Foxp3*$^{ERT2Cre+/y}$ mice with *Il1rl1*$^{fl/fl}$ animals, to delete ST2 on FOXP3-expressing Treg cells. After confirming that ST2 expression was deleted on both splenic and tissue Tregs prior to infection **(Fig S3G)** we intracranially infected mice with both intact (*Foxp3*$^{Ert2Cre+/y}$:: *Il1rl1*$^{fl/+}$) and deleted (*Foxp3*$^{Ert2Cre+/y}$:: *Il1rl1*$^{fl/fl}$) Treg ST2 with ZIKV-Dakar. Despite effective ST2 deletion on Tregs we observed no difference in survival **(Fig 3E)** or weight loss **(Fig S3H)** between groups, indicating that Treg expression of ST2 is dispensable for CNS flavivirus defense. As an alternative approach to assess a role for Tregs in survival following neuroinvasive WNV infection, we boosted the number and reactivity of Tregs via administration of IL-2 complexes [30] following CNS infection of WNV-E218A. While both the number of Tregs and expression of effector proteins CD25 and GITR were increased in circulation 9 DPI **(Figs S3I and S3J),** no effect of survival or weight loss to WNV-E218A infection was observed in response to IL-2 complex administration **(Fig S3K and S3L)**. Collectively, these data suggest that while ST2 expression is prominent on adaptive immune cells during peak CNS disease, signaling via the IL-33/ST2 axis on adaptive immune cells is dispensable for direct CNS immune responses to flaviviruses.

bioRxiv preprint doi: https://doi.org/10.1101/2023.04.11.536332; this version posted April 12, 2023. The copyright holder for this preprint (which was not certified by peer review) is the author/funder, who has granted bioRxiv a license to display the preprint in perpetuity. It is made available under aCC-BY 4.0 International license.

IL-33 signaling is required for normal microglial activation following neuroinvasive WNV infection

We next sought to identify an effector cell population for the IL-33/ST2 axis during CNS flavivirus infection. Given our negative findings regarding roles for lymphocytes in this process, as well as recent work highlighting a role for IL-33 signaling in microglial activation [6,7,31], we tested whether IL-33 release is associated with microglial activation in the CA3 region. To do this, we infected wild-type mice with increasing doses of WNV-E218A, then assessed both the number of IL-33-positive cells and microglial activation by staining for the macrophage somatic marker Iba1 and the phagosomal marker CD68. We observed that IL-33 staining decreased in both the pyramidal layer and stratum lucidi of the CA3 region with increasing infectious doses of WNV-E218A **(Figs 4A and 4B)**, consistent with IL-33 release in these regions. Furthermore, loss of IL-33 in both regions correlated with increased Iba1 while CD68 staining was also increased in both regions **(Figs 4A and 4B).**

These data suggested that IL-33/ST2 signaling may drive microglia activation following WNV infection. To test this more directly, we analyzed microglial activation by quantifying the MFI of the macrophage marker Iba1 by IHC in both WT and *Il1rl1*$^{-/-}$ mice 7 DPI with WNV-E218A. We observed a striking impairment of microglial activation 7 days post-infection in CA3, deep cerebellar nuclei (DCN), and cortex of *Il1rl1*$^{-/-}$ mice **(Figs 4C and 4D)**. Importantly, mock-infected B6/J and *Il1rl1*$^{-/-}$ mice did not differ in Iba1 MFI, indicating no baseline effect of IL-33 on Iba1 intensity **(Figs S4A and S4B).** Further, when we analyzed B6/J and *Il1rl1*$^{-/-}$ mice at 10 DPI, this activation phenotype was maintained,

bioRxiv preprint doi: https://doi.org/10.1101/2023.04.11.536332; this version posted April 12, 2023. The copyright holder for this preprint (which was not certified by peer review) is the author/funder, who has granted bioRxiv a license to display the preprint in perpetuity. It is made available under aCC-BY 4.0 International license.

suggesting IL-33 signaling may contribute to persistent microglial activation phenotypes post-infection **(Figs S4C and S4D)**. Despite its reported role in synaptic stripping by activated microglia in diverse CNS pathologies [32], complement deposition of C1q protein at 7DPI was not affected by the absence of IL-33 during infection **(Figs S4E and S4F).**

To directly test whether the loss of IL-33/ST2 signaling on microglia, and resulting impairment in activation, was responsible for the increased susceptibility to WNV infection we previously observed in IL-33- and ST2-deficient mice, we crossed *Cx3cr1*$^{\text{Ert2Cre}}$ mice with *Il1rl1*$^{fl/fl}$ animals. In resulting *Cx3cr1*$^{Ert2Cre/+}$*:: Il1rl1*$^{fl/fl}$ animals, tamoxifen administration causes ST2 excision in all tissue resident macrophages. However, we used a previously-defined strategy of administering tamoxifen, then resting mice for one month to allow turnover of peripheral, but not brain-resident, macrophage populations **(Goldmann et al., 2013)**. We first confirmed microglial ST2 excision in naïve mice one-month post tamoxifen treatment by MAC sorting whole brain homogenate with CD11b beads and subsequent RT-PCR. After first confirming purity of our samples by flow cytometry **(Figs S4G-S4H),** we observed downregulation of the ST2 receptor only in *Cx3cr1*$^{Ert2Cre/+}$*:: Il1rl1*$^{fl/fl}$ sorted microglia by RT-PCR **(Fig S4I).** Next, we infected tamoxifen-treated *Cx3cr1*$^{Ert2Cre/+}$*:: Il1rl1*$^{fl/fl}$ and *Cx3cr1*$^{+/+}$*:: Il1rl1*$^{fl/fl}$ animals intracranially with WNV-E218A and monitored their survival. While animals with intact ST2 signaling on brain macrophages survived at rates comparable to WT animals, *Cx3cr1*$^{\text{ERT2Cre/+}}$*:: Il1rl1*$^{fl/fl}$ mice displayed significantly increased mortality **(Fig 4E)** and weight loss (**Fig S4J**), comparable to that observed when this infection model was applied to mice globally lacking ST2 or IL-33 **(Fig. 1A).** A recent study identified ST2 expression on peripheral sensory neurons in the context of sterile skin injury [35]. To test whether neuronal ST2 expression contributed to

bioRxiv preprint doi: https://doi.org/10.1101/2023.04.11.536332; this version posted April 12, 2023. The copyright holder for this preprint (which was not certified by peer review) is the author/funder, who has granted bioRxiv a license to display the preprint in perpetuity. It is made available under aCC-BY 4.0 International license.

our phenotypes we crossed *Camk2a*$^{Cre/+}$ mice with *Il1rl1*$^{fl/fl}$ mice generating mice with intact (*Camk2a*$^{+/+}$*:: Il1rl1*$^{fl/fl}$) and deficient *(Camk2a*$^{Cre/+}$*: Il1rl1*$^{fl/fl}$*)* neuronal ST2 signaling. Upon WNV-E218A infection no change in survival (**Fig S4K**) or weight loss (**Fig S4L**) was seen. Together, these findings support the idea that ST2 expression on microglia is responsible for both macrophage activation and host survival in response to WNV infection.

Brain macrophages from *Il33*$^{-/-}$ mice exhibit enhanced inflammatory and stress responses post-infection

In light of these phenotypes and to identify the transcriptional programs initiated by IL-33 on brain macrophages following infection, we isolated hippocampal brain macrophages (a population expected to include both microglia and recruited peripheral monocyte-derived macrophages) using F4/80 mediated MACS from WT and *Il33*$^{-/-}$ mice 7 days after intracranial WNV-E218A infection and processed them for RNA sequencing. **(Fig 5A)**. Before sequencing, MAC-sorted sample purity was determined by flow cytometry**(Figs S5A-S5C).** Following RNAseq analysis, we first performed principal component analysis and observed clustering of samples by both genotype and infection status **(Fig 5B)**. Analysis of RNAseq datasets revealed 251 significantly differentially expressed genes when comparing B6/J and IL-33 deficient macrophages during infection **(Fig 5C)**. Additionally, and consistent with previous reports, we observed a number of differentially expressed genes in vehicle-treated IL-33-deficient animals relative to wild-type controls, consistent with homeostatic roles for IL-33 [31] **(Fig S5D)**. We next performed

bioRxiv preprint doi: https://doi.org/10.1101/2023.04.11.536332; this version posted April 12, 2023. The copyright holder for this preprint (which was not certified by peer review) is the author/funder, who has granted bioRxiv a license to display the preprint in perpetuity. It is made available under aCC-BY 4.0 International license.

Gene Set Enrichment Analysis (GSEA) using Hallmark gene sets that may be differentially expressed during infection. While the top gene sets enriched in IL-33-deficient cells relative to wild-type **(Fig 5D and S5E)** during infection included predictable dysregulation of inflammatory processes **(Figs S5D and S5F)**, we were surprised to observe a number of cell metabolism and stress gene sets enriched including: Fatty Acid Metabolism **(Fig S5G)**, Oxidative Phosphorylation **(Fig S5H)**, Hypoxia **(Fig S5I)** and Apoptosis **(Fig S5J).** Collectively, these data point to a dysregulation of brain macrophage activation following WNV-E218A infection in *Il33*$^{-/-}$ mice typified by altered metabolic state and upregulation of cell stress pathways, including apoptosis.

IL-33 functions as a microglial survival factor limiting CNS pathology following WNV infection

Previous studies have shown a role for IL-33 in the metabolic support of macrophage survival [5,31] . Since we observed a lack of macrophage activation and hypertrophy in ST2-deficient mice, as well as upregulated cell stress pathways in brain macrophages isolated from *Il33*$^{-/-}$ mice, we hypothesized that brain macrophage viability may be impacted subsequent to intracranial WNV-E218A delivery in the absence of IL-33/ST2 signaling. To quantify this, we examined brain macrophage (CD11b+F4/80+) viability in *Il1rl1*$^{-/-}$ mice post-infection by flow cytometry. Looking 7 days post-infection with WNV-E218A we observed that in whole brain samples, macrophages, but not other infiltrating leukocyte populations exhibited higher proportions of cell death as quantified by the viability dye ZombieNIR **(Fig 6A).** To confirm this phenotype, we next performed IHC on B6/J and *Il33*$^{-/-}$ mice infected with WNV-E218A at 7 days post infection, using the

bioRxiv preprint doi: https://doi.org/10.1101/2023.04.11.536332; this version posted April 12, 2023. The copyright holder for this preprint (which was not certified by peer review) is the author/funder, who has granted bioRxiv a license to display the preprint in perpetuity. It is made available under aCC-BY 4.0 International license.

macrophage marker Iba1 and terminal apoptotic marker cleaved-caspase 3 (CC3). We observed marked macrophage apoptosis in the CA3 of *Il33*$^{-/-}$ mice with WNV-E218A infection **(Figs 6B and 6C)** and also in hippocampal CA1 7 DPI with ZIKV-Dakar (**Figs S6A and S6B).**

A key driver of pathology in neuroinvasive WNV disease is the entry of peripheral monocytes to the CNS [36–38]. Given the blunted activation and enhanced apoptosis observed in resident microglia in the absence of IL-33/ST2 signaling, we wondered if peripheral monocytes would be recruited in greater numbers in these animals to compensate for—or in response to—dysregulated microglial responses. To assess this, we examined the number of brain-engrafted monocytes in B6/J and *Il1rl1*$^{-/-}$ by flow cytometry following intracranial WNV-E218A infection and observed a marked increase in the number of monocytes in whole brain homogenates **(Fig 6D)**. Enhanced monocyte engraftment post-infection was also corroborated by quantifying CD68+Iba1- cells in CA3 and cerebellum of B6/J and *Il33*$^{-/-}$ mice at 7DPI by immunohistochemistry of infected brain tissue (**Figs 6E and 6F**)

Given the strong phenotypes seen with both global and microglial deletion of IL-33 signaling on host and brain macrophage survival, we next sought to examine CNS pathologic processes that may underlie host demise. To examine neuronal pathology we stained hippocampal region CA3 and cerebellum in both B6/J and *Il33*$^{-/-}$ mice infected with WNV-E218A using antibodies against the neuronal distress marker phospho-c-Jun [39] and endogenous mouse IgG to mark blood-brain barrier (BBB) leakage. Strikingly, we saw an increase in CA3 IgG deposition and phospho-c-Jun+ cells in both areas of *Il1rl1*$^{-/-}$ animals **(Figs 6G and 6H)**. We also observed increased staining for the astrocyte

bioRxiv preprint doi: https://doi.org/10.1101/2023.04.11.536332; this version posted April 12, 2023. The copyright holder for this preprint (which was not certified by peer review) is the author/funder, who has granted bioRxiv a license to display the preprint in perpetuity. It is made available under aCC-BY 4.0 International license.

activation marker GFAP in these regions, as well as increased phospho-c-Jun expression in mossy fibers of CA3 of *Il1rl1*$^{-/-}$ animals, an early phenotype of neurodegeneration observed in many models of CNS pathology [40] (**Figs 6I and 6J**). Collectively these data are consistent with a state of increased monocyte ingress and vascular leak, neuronal distress, and astrocyte hyperactivity in *Il33*$^{-/-}$ mice following flavivirus infection.

Lastly, we examined apoptotic neurons in hippocampal CA3 and cerebellum by quantifying cleaved-caspase 3 positive NeuN expressing cells and found increased neuronal apoptosis in *Il33*$^{-/-}$ mice at 7 DPI in both regions **(Figs 6K and 6L)**. Together, these data suggest that IL-33/ST2 signaling is required during intracranial flavivirus infection to promote microglial viability. Our findings indicate that in the absence of IL-33 signaling, flavivirus infection leads to microglial apoptosis, ingress of pathogenic, peripheral monocyte-derived cells to the CNS, neuronal distress, astrocyte hyperactivity, and subsequent enhanced neuronal apoptosis and host demise.

Discussion

This study defines IL-33 as an oligodendrocyte-derived survival factor for microglia, and suggests that IL-33 is required during viral infection to promote normal microglial activation. In its absence, we observed wide-ranging defects in neuronal survival, blood-brain barrier integrity, and peripheral monocyte infiltration, culminating in reduced host survival. While the work detailed here does not define a mechanism for oligodendrocyte release of IL-33, previous studies have demonstrated profound WNV-induced death of oligodendrocytes *in vitro,* [20], from cultured explants [21]**,** and *in vivo* during peripheral infection [22]**.** While these studies mainly indicated apoptotic death of oligodendrocytes,

bioRxiv preprint doi: https://doi.org/10.1101/2023.04.11.536332; this version posted April 12, 2023. The copyright holder for this preprint (which was not certified by peer review) is the author/funder, who has granted bioRxiv a license to display the preprint in perpetuity. It is made available under aCC-BY 4.0 International license.

other works have shown that oligodendrocytes express low levels of caspase 8 [41], a mediator of death-receptor induced apoptosis, and that TNF is a robust inducer of oligodendrocyte necrosis/necroptosis [42], implying that oligodendrocytes may be poised for pro-inflammatory cell death, especially during viral infection. These data, in addition to the finding that IL-33 reactivity is reduced, but not eliminated, by caspase 7 during apoptosis [43] suggests that oligodendrocytes may undergo non-apoptotic cell death to release IL-33 during neurotropic viral infection. Future studies will define the inducers and mechanisms underlying these effects.

Our work also indicates that IL-33 signaling on adaptive immune populations does little to affect survival at least in direct intracranial infection of flaviviruses. This is despite our observation that ST2 expression was most widely seen on adaptive immune populations at either resting state or during peak infection. This may be attributable to reports that ST2 expression on various immune cells is very short-lived , as in the case of splenic CD8 T cells in LCMV infection [23], or can shift in response to inflammatory context such as its upregulation on macrophages and Natural Killer cells in models of airway smoke exposure [44]. Despite observing limited ST2 expression on microglia, ST2 deletion on microglial cells did impact survival phenotypes in a manner similar to germline knockout of ST2. Still, future studies may need to employ multiple timepoints, possibly on an hourly timescale, to detect ST2 expression by protein on microglia.

While our studies observed enhanced expression of inflammatory and cell stress gene sets on microglial populations in response to WNV infection, we were technically limited in our sorting of F4/80+ cells, which at 7 DPI include both microglia and engrafted monocyte-derived macrophages. Future experiments delineating resident microglia via

bioRxiv preprint doi: https://doi.org/10.1101/2023.04.11.536332; this version posted April 12, 2023. The copyright holder for this preprint (which was not certified by peer review) is the author/funder, who has granted bioRxiv a license to display the preprint in perpetuity. It is made available under aCC-BY 4.0 International license.

genetic fate-mapping and crossing to appropriate knockout strains may be required, as no definitive microglial marker separating these cell types in disease states currently exists.

Notably, the effect of IL-33 on host defense was not due to a failure of viral clearance, as mice deficient in IL-33 signaling had equivalent viral titers at peak disease timepoints and those that survived acute infection eventually cleared virus from CNS tissues. Previous data have indicated a requirement for microglia in CNS WNV infection, with deletion pharmacologically [16] or genetically [18] yielding decreased host survival. However, the CNS of mice with pharmacologic microglial depletion also showed higher levels of infectious virus and a blunted adaptive immune response, contrary to what was observed here. This suggests that IL-33 signaling may drive a subset of microglial functions related to survival and disease tolerance in the context of viral infection, and that in its absence microglia may still participate in viral control. There may also be differences between genetic and pharmacological depletion of microglia, as WNV-E218A infection of microglia-deficient *Il34*$^{-/-}$ mice revealed decreased neuronal and host survival with no change to CNS viral titer [18], similar to our data.

While the presence of microglia within the virally-infected CNS is clearly beneficial for host and neuronal survival, how are microglia providing their neuroprotective effect independent of effects on viral titer? The provision of secreted factors by microglia to neurons directly or through supporting cells is one obvious possibility. Both TGF-β and IGF-1 have been shown to be secreted by microglia during spinal cord injury and observed to promote neuronal survival at the injury site [45]**.** The anti-inflammatory cytokine IL-10, which is secreted by microglia in response to bacterial infection [46] may also be

bioRxiv preprint doi: https://doi.org/10.1101/2023.04.11.536332; this version posted April 12, 2023. The copyright holder for this preprint (which was not certified by peer review) is the author/funder, who has granted bioRxiv a license to display the preprint in perpetuity. It is made available under aCC-BY 4.0 International license.

416 responsible for tuning the CNS inflammatory milieu and ensuring neuroprotection.
417 Another possibility is microglial secretion of brain-derived neurotrophic factor (BDNF)
418 which is elicited by microglia during models of nerve injury and alters neuronal activity [47].
419 Microglial neuroprotection may also be mediated by synaptic stripping, preventing
420 aberrant neuronal activity at sites of infection from "spillover" to otherwise healthy
421 neuronal tissue.

422 IL-33 has recently emerged as a critical factor mediating macrophage survival in
423 multiple settings. For example, IL-33 signaling was shows to promote survival in red pulp
424 macrophage development [5] as well as altering microglial metabolic functioning [31]. Our
425 findings join other recent studies implicating IL-33 signaling on microglia as essential to
426 tune CNS function during development [6] and in adulthood [7]**.** In implicating IL-33 as a
427 promoter of microglia-mediated disease tolerance (rather than a driver of viral clearance
428 [48,49]) our findings highlight the pleotropic functions of microglia in both homeostasis and
429 disease. Our work also suggests that potentiating IL-33 signaling in the CNS could
430 ameliorate pathology and sequelae associated with neurotropic flavivirus infection.

431

432 **Materials and Methods**

433 **Mice**

434

435 B6/J (000664), *Il33*$^{fl/fl}$ (030619) *Cx3cr1*$^{ERT2Cre/\ ERT2Cre}$ (020940), *Plp1*$^{ERT2Cre/ERT2Cre}$
436 (005975), Aldh1l1$^{ERT2cre/\ ERT2cre}$ (029655), and *Camk2a*$^{Cre/Cre}$ (005359) mice were obtained
437 from Jackson Laboratories. C57BL/6J (B6/J) controls were either obtained commercially
438 (Jackson Laboratories) or, for control animals in experiments using transgenic mouse

bioRxiv preprint doi: https://doi.org/10.1101/2023.04.11.536332; this version posted April 12, 2023. The copyright holder for this preprint (which was not certified by peer review) is the author/funder, who has granted bioRxiv a license to display the preprint in perpetuity. It is made available under aCC-BY 4.0 International license.

strains, WT mice were bred in-house. *Il33*$^{-/-}$ (Originally from Dirk Smith at Amgen) and Foxp3$^{ERT2Cre/y}$ (PMID: 18387831):: *Il1rl1*$^{fl/fl}$ mice were obtained from the Ziegler lab (Benaroya Research Institute). *Il1rl1*$^{-/-}$ (ST2$^{-/-}$) (PMID: 10727469) mice were provided by the Von Moltke lab (University of Washington). Mice in this study were bred and housed under specific-pathogen free conditions at the University of Washington.

Tamoxifen and in vivo injections

To induce Cre activity in Cre-ERT2 mice, 100 uL of Tamoxifen (Sigma) at 20 mg/mL dissolved in corn oil (Sigma) was injected every day for 5 consecutive days with mice analyzed one month later. For CD8 T cell depletion mice were injected on days -1, 2, 5, and 8 post-infection with 200 ug of αCD8 (Clone 2.43 BioXcell) or control IgG antibody in 200 uL PBS (PMID: 30143586). Depletion was confirmed by obtaining blood from the retro orbital sinus 6DPI. To induce Treg expansion (PMID: 30291203) the JES6-1 αIL-2 antibody was mixed at a 2:1 molar ratio with IL-2 for 30 minutes at 37^0 C in PBS. Mice were injected daily with a complex of 1 ug IL-2 (Peprotech) and 5 ug JES6-1 (BioXcell) intraperitoneally on days 2-4 post-infection in a total volume of 200 uL. Expansion was confirmed by obtaining blood from the retro orbital sinus at 9DPI.

Viruses

WNV-Tx was provided by Mike Gale of the University of Washington. WNV-E218A and ZIKV-Dakar strains utilized for intracranial infections were obtained from Robyn Klein at

bioRxiv preprint doi: https://doi.org/10.1101/2023.04.11.536332; this version posted April 12, 2023. The copyright holder for this preprint (which was not certified by peer review) is the author/funder, who has granted bioRxiv a license to display the preprint in perpetuity. It is made available under aCC-BY 4.0 International license.

Washington University in St Louis. WNV-NS5-E218A contains a single point mutation in the gene encoding 2′-*O*-methyltransferase (PMID: 31611100). Mice were deeply anesthetized and intracranially administered 2e4 plaque-forming units (p.f.u.) of WNV-NS5-E218A or 1e6 PFU of ZIKV-Dakar as described previously (PMID: 31235930). Viruses were diluted in 20 µl of Hank's balanced salt solution (HBSS) and injected into the third ventricle of the brain with a guided 29-guage needle. Mock-infected mice were intracranially injected with 20 µl of HBSS. Footpad infections were performed by injection of 100 PFU WNV in 50 µL of HBSS into a rear footpad as previously described (PMID: 28366204). BHK21 cells were used for quantification of WNV Titers while Vero cells were used for titering ZIKV-Dakar as described (PMID: 24510289).

Infected mice were monitored daily for weight loss and presentation of clinical signs of disease, including hunched posture, ruffled fur, hindlimb weakness, and paresis. Severity of paresis was defined as follows: mild – partial loss of motor function in one hind limb; moderate – com- plete or nearly complete loss of motor function in one hind limb or partial loss of motor function in both hind limbs; severe – complete or nearly complete loss of motor function in both hind limbs and/or pronounced ataxia. Mice reaching a moribund state or losing more than 30% of initial body weight were euthanized as performed previously (PMID:28366204). All experiments were performed in both male and female 2-4 month old mice, in accordance with protocols approved by the University of Washington Animal Care and Use Committee (IACUC).

Measurement of viral burden

bioRxiv preprint doi: https://doi.org/10.1101/2023.04.11.536332; this version posted April 12, 2023. The copyright holder for this preprint (which was not certified by peer review) is the author/funder, who has granted bioRxiv a license to display the preprint in perpetuity. It is made available under aCC-BY 4.0 International license.

WNV- or ZIKV-infected mice were sacrificed and tissues were collected, weighed, and homogenized with Precellys zirconia beads in a Precellys 24 homogenizer in 500 µl of PBS, and stored at –80 °C until virus titration. Thawed samples were clarified by centrifugation (2,000 × g at 4 °C for 10 min), and then diluted serially before infection of BHK21 cells for WNV or Vero cells for ZIKV titers. Plaque assays were overlaid with low-melting point agarose, fixed 4 days later with 4% formaldehyde, and stained with crystal violet. Viral burden was expressed on a $\log_{10}$ scale as p.f.u. per gram of tissue.

Tissue preparation and CNS leukocyte isolation

All tissues harvested from mice for subsequent immunohistochemical, MACs, qRT-PCR, protein, virologic, or flow cytometric analysis were extracted following extensive cardiac perfusion with 10 mL of sterile PBS after cutting the right atrium. For flow cytometry and MACs, leukocytes were isolated from whole brains after digestion in 0.05% collagenase A (Sigma-Aldrich) and 10 mg/ml DNase I (Sigma- Aldrich), then purified via centrifugation in 37% isotonic Percoll (Sigma-Aldrich) as described (PMID: 22729249). For MACs cells were incubated with anti-F4/80 microbeads (Miltenyi) and separated with LS columns (Miltenyi) per manufacturer's recommendations. FACs was performed on an LSRII (Becton Dickinson) with analysis completed on FlowJo (Becton Dickinson).

Immunofluorescence and FACs antibodies

bioRxiv preprint doi: https://doi.org/10.1101/2023.04.11.536332; this version posted April 12, 2023. The copyright holder for this preprint (which was not certified by peer review) is the author/funder, who has granted bioRxiv a license to display the preprint in perpetuity. It is made available under aCC-BY 4.0 International license.

Brain tissue was fixed for 48 h in 4% PFA, followed by cryoprotection in 30% sucrose for 48 h. Brains were then frozen in optimal cutting temperature compound (Tissue-Tek) on the freezing element of a Leica CM3050 S cryostat. 40-µm sections were sliced into 24-well plates containing PBS with 0.05% sodium azide as previously described (PMID: 29941548). Slices were permeabilized and blocked with 0.25% Triton X-100 and 5% Normal Donkey Serum (Sigma) for 1 hour followed by overnight incubation in 0.5% BSA with primary antibody at 4° C. The following antibodies were used for immunofluorescence staining: rabbit anti-Iba1 (1:300; CP-290; Biocare Medical), Goat anti-Iba1(1:300; Abcam; ab5076), rat anti-CD68 (1:300; FA-11; Biolegend), Goat anti-IL-33 (AF3626; R&D), Rabbit anti-Olig2 (1:500; AB 9610; Millipore Sigma), Rat-anti GFAP (1:2000; 2.2B10; Thermo Fischer Scientific), Rabbit anti-Sox9 (1:500; AB5535; EMD Millipore), Rabbit anti-NeuN (1:2000; D3S3I; Cell Signaling), Chicken anti-NeuN (1:300; 266 006; Synaptic Systems), Rabbit anti-C1q (1:300; ab182451; Abcam), Rabbit anti-Cleaved caspase three (1:500; ab9661; Cell-Signaling), Rabbit anti-Phospho-c-Jun (1:1000; D47G9; Cell Signaling), and Donkey anti-Mouse IgG (1:2000; A21203; Life Technologies) . Slices were washed three times for 5 min, incubated for 2 h at room temperature with the appropriate secondary antibodies (all Donkey-derived from Thermo Fisher or Jackson Immunology using Alexaflours 488, 594, and 647; Life Technologies; 1:1,000), washed in PBS with DAPI (1:20,000; 62248; Thermo Fischer Scientific) washed again three times for 5 min and mounted with Aquamount (14-390-5; Thermo Fischer Scientific). Blinded image analysis including cell counting and MFI calculations were all performed with ImageJ (National Institutes of Health).

bioRxiv preprint doi: https://doi.org/10.1101/2023.04.11.536332; this version posted April 12, 2023. The copyright holder for this preprint (which was not certified by peer review) is the author/funder, who has granted bioRxiv a license to display the preprint in perpetuity. It is made available under aCC-BY 4.0 International license.

Antibody cocktails for FACs staining were used at 1:100 in 2 mM EDTA (15-575-020; Fischer Scientific) and 0.5% BSA (A7906-100G) or FOXP3/ Transcription Factor buffers (00-5523-00; eBioscience) when staining for FOXP3. Antibodies used included GLAST (130-123-555; Miltenyi), biotinylated ST2 (101001B; MD Bioscience), Streptavidin R-Phycoerythrin (S21338; Thermo Scientific) and PE-conjugated NS4b tetramers (Fred Hutch antibody core). Antibodies against CD3 (17A2; Fischer Scientific), CD4 (RM-4; Fischer Scientific), CD8 (53-6.7; Fischer Scientific), CD44 (IM7; Fischer Scientific), CD69 (H1.2F3; Fischer Scientific), FOXP3 (FJK-16s; Fischer Scientific), F4/80 (T45-2342; Fischer Scientific), NK1.1 (PK136; BioLegend), CD19 (1d3; Thermo Fisher), Ly6C (AL-21; Fischer Scientific), Ly6G (1A8; Fischer Scientific), GITR (DTA-1; Fischer Scientific), and CD25 (PC61; Fischer Scientific).

Statistical analyses

Statistical analyses comparing two groups at one time point were done using a student's t-test in Prism software, v. 7.0a. One-way and two-way ANOVA were used appropriately and were indicated. The number of mice per group, test used, and p values are denoted in each Fig legend. Data was graphed using Prism software, v9 (GraphPad).

Macrophage preparation and RNAsequencing

After MACs isolation, brain macrophages were washed in PBS and cell pellets prepared using the RNAqueous Micro kit (Ambion) per manufacturer's instruction. Total RNA was

bioRxiv preprint doi: https://doi.org/10.1101/2023.04.11.536332; this version posted April 12, 2023. The copyright holder for this preprint (which was not certified by peer review) is the author/funder, who has granted bioRxiv a license to display the preprint in perpetuity. It is made available under aCC-BY 4.0 International license.

concentrated by evaporation using an Eppendorf Vacufuge system and was then added to lysis buffer from the SMART-Seq v4 Ultra Low Input RNA Kit for Sequencing (Takara). Reverse transcription was performed followed by 20 cycles of PCR amplification to generate full length amplified cDNA. Sequencing libraries were constructed using the NexteraXT DNA sample preparation kit with unique dual indexes (Illumina) to generate Illumina-compatible barcoded libraries. Libraries were pooled and quantified using a Qubit® Fluorometer (Life Technologies). Sequencing of pooled libraries was carried out on a NextSeq 2000 sequencer (Illumina) with paired-end 59-base reads, using a NextSeq P3 sequencing kit (Illumina) with a target depth of 5 million reads per sample. Base calls were processed to FASTQs on BaseSpace (Illumina), and a base call quality-trimming step was applied to remove low-confidence base calls from the ends of reads. The FASTQs were aligned to the GRCm38 mouse reference genome, using the STAR aligner, and gene counts were generated using htseq-count. QC and metrics analysis was performed using the Picard family of tools (v1.134).

Following generation of the counts matrix analyses were performed using R (v4.2.2). The flow of analyses began with PCA analysis and visualization using the PCAtools package (v2.10). Normalization and differential gene expression testing analyses were performed using the DESeq2 package (v1.38.3) using the Wald statistical testing method applied two condition comparisons. The DESeq2 results were then used to generate ranks for gene set enrichment analysis (GSEA) using the fgsea package (v1.24.0) to test for enrichment of gene ontology terms using the mouse ontology gene sets (M5) collection downloaded from gsea-msigdb. The results from the GSEA and differential gene expression testing were visualized using a combination of the ggplot2

bioRxiv preprint doi: https://doi.org/10.1101/2023.04.11.536332; this version posted April 12, 2023. The copyright holder for this preprint (which was not certified by peer review) is the author/funder, who has granted bioRxiv a license to display the preprint in perpetuity. It is made available under aCC-BY 4.0 International license.

(v3.4.0), pheatmap (v1.0.12), and EnhancedVolcano (v1.16.0) packages. All code relevant to the data analyses in this study are available online at https://github.com/OberstLab. The software used for the R analyses are publicly available.

Acknowledgments

We thank Pooja Jain and Valerie Sheehan for technical assistance. We thank the lab of Dr. Michael Gale, Jr., at the University of Washington for technical assistance and discussion. We thank the viviarium staff of the University of Washington Department of Comparative Medicine SLU 3.1 for their help and support. We thank all members of the Oberst Lab for their input and support. We thank the Von Moltke and Pepper labs of the University of Washington and the Ziegler lab of Benaroya Research Institute for mouse lines used in this study. This work was supported by NIH/NIAID grants R01 AI132595 and R21 AI178512 to AO. JMA was supported by the Helen Hay Whitney Foundation.

Author Contributions

Conceptualization: GTN, JMA, AO; Methodology: GTN, JMA, AO; Analysis: GTN, AO (all), JMA (RNAseq data analysis); Investigation: GTN (all), JMA (RNAseq experimental workflow); Resources: AO, SFZ; Writing-Original draft: GTN, AO; Writing-review and editing: All authors.

Declarations of Interest

bioRxiv preprint doi: https://doi.org/10.1101/2023.04.11.536332; this version posted April 12, 2023. The copyright holder for this preprint (which was not certified by peer review) is the author/funder, who has granted bioRxiv a license to display the preprint in perpetuity. It is made available under aCC-BY 4.0 International license.

The authors declare no competing interests.

References

1. Chakarov S, Ginhoux F, Ble C. Review Determinants of Resident Tissue Macrophage Identity and Function. 2020:957-970. doi:10.1016/j.immuni.2020.05.014
2. Wolf SA, Boddeke HWGM, Kettenmann H. Microglia in Physiology and Disease. *Annu Rev Physiol*. 2017;79:619-643. doi:10.1146/annurev-physiol-022516-034406
3. Prinz M, Masuda T, Wheeler MA, Quintana FJ. Microglia and Central Nervous System-Associated Macrophages mdash from Origin to Disease Modulation. *Annu Rev Immunol*. 2021;39:251-277. doi:10.1146/annurev-immunol-093019-110159
4. Klein RS, Garber C, Funk KE, et al. Neuroinflammation During RNA Viral Infections. *Annu Rev Immunol*. 2019;37(1):73-95. doi:10.1146/annurev-immunol-042718-041417
5. Lu Y, Basatemur G, Scott IC, et al. Interleukin-33 Signaling Controls the Development of Iron-Recycling Macrophages. *Immunity*. 2020;52(5):782-793.e5. doi:10.1016/j.immuni.2020.03.006
6. Vainchtein ID, Chin G, Cho FS, et al. Astrocyte-derived interleukin-33 promotes microglial synapse engulfment and neural circuit development. *Science*. 2018:1-8.
7. Nguyen PT, Dorman LC, Pan S, et al. Microglial Remodeling of the Extracellular Matrix Promotes Synapse Plasticity. *Cell*. 2020;182(2):388-403.e15.

bioRxiv preprint doi: https://doi.org/10.1101/2023.04.11.536332; this version posted April 12, 2023. The copyright holder for this preprint (which was not certified by peer review) is the author/funder, who has granted bioRxiv a license to display the preprint in perpetuity. It is made available under aCC-BY 4.0 International license.

doi:10.1016/j.cell.2020.05.050

8. Gadani SP, Walsh JT, Smirnov I, Zheng J, Kipnis J. The Glia-Derived Alarmin IL-33 Orchestrates the Immune Response and Promotes Recovery following CNS Injury. *Neuron*. 2015;85(4):703-709. doi:10.1016/j.neuron.2015.01.013

9. Still KM, Batista SJ, O'Brien CA, et al. Astrocytes promote a protective immune response to brain Toxoplasma gondii infection via IL-33-ST2 signaling. *PLoS Pathog*. 2020;16(10):1-28. doi:10.1371/journal.ppat.1009027

10. Garber C, Vasek MJ, Vollmer LL, Sun T, Jiang X, Klein RS. Astrocytes decrease adult neurogenesis during virus-induced memory dysfunction via IL-1 article. *Nat Immunol*. 2018;19(2):151-161. doi:10.1038/s41590-017-0021-y

11. Collins MH, Metz SW. Progress and Works in Progress: Update on Flavivirus Vaccine Development. *Clin Ther*. 2017;39(8):1519-1536. doi:10.1016/j.clinthera.2017.07.001

12. Petersen LR, Brault AC, Nasci RS. West Nile virus: Review of the literature. *JAMA - J Am Med Assoc*. 2013;310(3):308-315. doi:10.1001/jama.2013.8042

13. Gould E, Solomon T. Pathogenic flaviviruses. *Lancet*. 2008;371(9611):500-509. doi:10.1016/S0140-6736(08)60238-X

14. Vasek MJ, Garber C, Dorsey D, et al. A complement–microglial axis drives synapse loss during virus-induced memory impairment. *Nature*. 2016;534(7608):538-543. doi:10.1038/nature18283

15. Garber C, Soung A, Vollmer LL, et al. T cells promote microglia-mediated synaptic elimination and cognitive dysfunction during recovery from neuropathogenic flaviviruses. *Nat Neurosci*. 2019. doi:10.1038/s41593-019-0427-

bioRxiv preprint doi: https://doi.org/10.1101/2023.04.11.536332; this version posted April 12, 2023. The copyright holder for this preprint (which was not certified by peer review) is the author/funder, who has granted bioRxiv a license to display the preprint in perpetuity. It is made available under aCC-BY 4.0 International license.

y

16. Funk KE, Klein RS. CSF1R antagonism limits local restimulation of antiviral CD8 + T cells during viral encephalitis. 2019;4:1-19.

17. Klein RS, Garber C, Howard N. Infectious immunity in the central nervous system and brain function. *Nat Immunol*. 2017;18(2):132-141. doi:10.1038/ni.3656

18. Wang Y, Szretter KJ, Vermi W, et al. IL-34 is a tissue-restricted ligand of CSF1R required for the development of Langerhans cells and microglia. *Nat Immunol*. 2012;13(8):753-760. doi:10.1038/ni.2360

19. Szretter KJ, Daniels BP, Cho H, et al. 2′-O methylation of the viral mRNA cap by West Nile virus evades Ifit1-dependent and -independent mechanisms of host restriction in vivo. *PLoS Pathog*. 2012;8(5). doi:10.1371/journal.ppat.1002698

20. Jordan I, Briese T, Fischer N, Lau JY, Lipkin WI. Ribavirin Inhibits West Nile Virus Replication and Cytopathic Effect in Neural Cells. *J Infect Dis*. 2000;182(4):1214-1217. doi:10.1086/315847

21. Schultz V, Cumberworth SL, Gu Q, et al. Zika virus infection leads to demyelination and axonal injury in mature cns cultures. *Viruses*. 2021;13(1). doi:10.3390/v13010091

22. Schultz V, Barrie JA, Donald CL, et al. Oligodendrocytes are susceptible to Zika virus infection in a mouse model of perinatal exposure: Implications for CNS complications. *Glia*. 2021;69(8):2023-2036. doi:10.1002/glia.24010

23. Bonilla W V, Fröhlich A, Senn K, et al. The Alarmin Interleukin-33 Drives Protective Antiviral CD8+ TCell Responses. *Science (80-)*. 2012;(February). doi:10.1126/science.1215418

bioRxiv preprint doi: https://doi.org/10.1101/2023.04.11.536332; this version posted April 12, 2023. The copyright holder for this preprint (which was not certified by peer review) is the author/funder, who has granted bioRxiv a license to display the preprint in perpetuity. It is made available under aCC-BY 4.0 International license.

24. Baumann C, Bonilla W V., Fröhlich A, et al. T-bet– and STAT4–dependent IL-33 receptor expression directly promotes antiviral Th1 cell responses. *Proc Natl Acad Sci*. 2015;112(13):4056-4061. doi:10.1073/pnas.1418549112

25. Popovic B, Golemac M, Podlech J, et al. IL-33/ST2 pathway drives regulatory T cell dependent suppression of liver damage upon cytomegalovirus infection. *PLoS Pathog*. 2017;13(4):1-23. doi:10.1371/journal.ppat.1006345

26. Slon Campos JL, Mongkolsapaya J, Screaton GR. The immune response against flaviviruses. *Nat Immunol*. 2018. doi:10.1038/s41590-018-0210-3

27. Lanteri MC, O'Brien KM, Purtha WE, et al. Tregs control the development of symptomatic West Nile virus infection in humans and mice. *J Clin Invest*. 2009;119(11):3266-3277. doi:10.1172/JCI39387

28. Shrestha B, Diamond M. Role of CD8+ T cells in control of West Nile virus infection. *J Virol*. 2004;78(15):8312-8321. doi:10.1128/JVI.78.15.8312

29. Gadani SP, Smirnov I, Smith AT, Overall CC, Kipnis J. Characterization of meningeal type 2 innate lymphocytes and their response to CNS injury. *J Exp Med*. 2016:1-14.

30. Webster KE, Walters S, Kohler RE, et al. In vivo expansion of T reg cells with IL-2-mAb complexes: induction of resistance to EAE and long-term acceptance of islet allografts without immunosuppression. *J Exp Med*. 2009;206(4):751-760. doi:10.1084/jem.20082824

31. He D, Xu H, Zhang H, Rozenblatt-Rosen O, Regev A, Kuchroo VK. Disruption of the IL-33-ST2-AKT signaling axis impairs neurodevelopment by inhibiting microglial metabolic adaptation and phagocytic function. *Immunity*. 2022:1-15.

bioRxiv preprint doi: https://doi.org/10.1101/2023.04.11.536332; this version posted April 12, 2023. The copyright holder for this preprint (which was not certified by peer review) is the author/funder, who has granted bioRxiv a license to display the preprint in perpetuity. It is made available under aCC-BY 4.0 International license.

doi:10.1016/j.immuni.2021.12.001

32. Stephan AH, Barres B a., Stevens B. The Complement System: An Unexpected Role in Synaptic Pruning During Development and Disease. *Annu Rev Neurosci*. 2012;35(1):369-389. doi:10.1146/annurev-neuro-061010-113810

33. Goldmann T, Wieghofer P, Müller PF, et al. A new type of microglia gene targeting shows TAK1 to be pivotal in CNS autoimmune inflammation. *Nat Neurosci*. 2013;16(11):1618-1626. doi:10.1038/nn.3531

34. Norris GT, Smirnov I, Filiano AJ, et al. Neuronal integrity and complement control synaptic material clearance by microglia after CNS injury. 2018;215(7). doi:10.1084/jem.20172244

35. Liu B, Tai Y, Achanta S, et al. IL-33/ST2 signaling excites sensory neurons and mediates itch response in a mouse model of poison ivy contact allergy. *Proc Natl Acad Sci*. 2016;113(47):E7572-E7579. doi:10.1073/pnas.1606608113

36. Getts MT, Müller M, Rana S, et al. Ly6c + “inflammatory monocytes” are microglial precursors recruited in a pathogenic manner in West Nile virus encephalitis . *J Exp Med*. 2008;205(10):2319-2337. doi:10.1084/jem.20080421

37. Terry RL, Getts DR, Deffrasnes C, van Vreden C, Campbell IL, King NJC. Inflammatory monocytes and the pathogenesis of viral encephalitis. *J Neuroinflammation*. 2012;9:1-10. doi:10.1186/1742-2094-9-270

38. Getts DR, Terry RL, Getts MT, et al. Targeted blockade in lethal West Nile virus encephalitis indicates a crucial role for very late antigen (VLA)-4-dependent recruitment of nitric oxide-producing macrophages. *J Neuroinflammation*. 2012;9:2-9. doi:10.1186/1742-2094-9-246

bioRxiv preprint doi: https://doi.org/10.1101/2023.04.11.536332; this version posted April 12, 2023. The copyright holder for this preprint (which was not certified by peer review) is the author/funder, who has granted bioRxiv a license to display the preprint in perpetuity. It is made available under aCC-BY 4.0 International license.

39. Yarza R, Vela S, Solas M, Ramirez MJ. c-Jun N-terminal kinase (JNK) signaling as a therapeutic target for Alzheimer's disease. *Front Pharmacol*. 2016;6(JAN):1-12. doi:10.3389/fphar.2015.00321

40. Manning AM, Davis RJ. Targeting JNK for therapeutic benefit: From junk to gold? *Nat Rev Drug Discov*. 2003;2(7):554-565. doi:10.1038/nrd1132

41. Zhang Y, Chen K, Sloan S a., et al. An RNA-Sequencing Transcriptome and Splicing Database of Glia, Neurons, and Vascular Cells of the Cerebral Cortex. *J Neurosci*. 2014;34(36):11929-11947. doi:10.1523/JNEUROSCI.1860-14.2014

42. Ofengeim D, Ito Y, Najafov A, et al. Activation of necroptosis in multiple sclerosis. *Cell Rep*. 2015;10(11):1836-1849. doi:10.1016/j.celrep.2015.02.051

43. Lüthi AU, Cullen SP, McNeela EA, et al. Suppression of Interleukin-33 Bioactivity through Proteolysis by Apoptotic Caspases. *Immunity*. 2009;31(1):84-98. doi:10.1016/j.immuni.2009.05.007

44. Kearley J, Silver JS, Sanden C, et al. Cigarette smoke silences innate lymphoid cell function and facilitates an exacerbated type I interleukin-33-dependent response to infection. *Immunity*. 2015;42(3):566-579. doi:10.1016/j.immuni.2015.02.011

45. Bellver-Landete V, Bretheau F, Mailhot B, et al. Microglia are an essential component of the neuroprotective scar that forms after spinal cord injury. *Nat Commun*. 2019;10(1). doi:10.1038/s41467-019-08446-0

46. Rasley A, Tranguch SL, Rati DM, Marriot I. Murine Glia Express the Immunosuppressive Cytokine, Interleukin-10, Following Exposure to Borrelia burgdorferi or Neisseria meningitidis. *Glia*. 2006;479(March):132. doi:10.1002/glia

bioRxiv preprint doi: https://doi.org/10.1101/2023.04.11.536332; this version posted April 12, 2023. The copyright holder for this preprint (which was not certified by peer review) is the author/funder, who has granted bioRxiv a license to display the preprint in perpetuity. It is made available under aCC-BY 4.0 International license.

47. Trang T, Beggs S, Salter MW. Brain-derived neurotrophic factor from microglia: A molecular substrate for neuropathic pain. *Neuron Glia Biol*. 2012;7(1):99-108. doi:10.1017/S1740925X12000087

48. Medzhitov R, Schneider DS, Soares MP. Disease Tolerance as a Defense Strategy. *Science (80-)*. 2012;335(6071):165-184. doi:10.1126/science.1214935.Disease

49. Ayres JS. The Biology of Physiological Health. *Cell*. 2020;181(2):250-269. doi:10.1016/j.cell.2020.03.036

Figure Legends

Fig 1. The IL-33 pathway promotes survival upon neuroinvasive flavivirus infection, independent of viral control

(A) Survival analysis in *Il33*$^{-/-}$, *Il1rl1*$^{-/-}$, and B6/J mice following intracranial infection with 2e4 PFU WNV-E218A.

(B) WNV Viral titers from indicated CNS components and tissues of mice 7 days post-infection via plaque assay on BHK cells.

(C) Survival analysis in *Il33*$^{-/-}$, *Il1rl1*$^{-/-}$, and B6/J mice following intracranial infection of 1e6 PFU ZIKV-Dakar.

(D) ZIKV Viral titers from indicated CNS components and tissues of mice 7 days post-infection via plaque assay on Vero cells.

(E) WNV Viral titers from indicated CNS components and tissues of mice 10 days post-infection via plaque assay on BHK cells

bioRxiv preprint doi: https://doi.org/10.1101/2023.04.11.536332; this version posted April 12, 2023. The copyright holder for this preprint (which was not certified by peer review) is the author/funder, who has granted bioRxiv a license to display the preprint in perpetuity. It is made available under aCC-BY 4.0 International license.

Data are representative of 3 pooled independent experiments (error bars, SEM). * $p < 0.05$, ** $p < 0.01$, *** $p < 0.001$ (A, C) (Gehan-Breslow-Wilcoxon test) (B, D, E) (2-way ANOVA with Holm-Sidak Multiple comparisons).

Fig 2. Oligodendrocyte-derived IL-33 promotes survival to neurotropic flavivirus infection

(A) Ratios of IL-33+ cells in indicated brain regions in adult B6/J mice with HBSS injection.

(B) Representative immunofluorescent images of IL-33+ cell loss in B6/J Hippocampal CA3 7 days post intracranial infection with WNV-E218A (20x magnification, scale bars, 100 microns). Arrowheads indicate IL-33+Olig2+ and arrows IL-33+GFAP+ cells.

(C) Quantification of IL-33 positivity in Olig2+ and GFAP+ in B6/J Hippocampal CA3 7 days post intracranial infection with WNV-E218A.

(D) Representative images of Olig2+ cell loss in indicated brain regions 7 days post intracranial infection with WNV-E218A (20x magnification, scale bars, 100 microns).

(E) Quantification of Olig2+ cell number in Hippocampal CA3 7 days post intracranial infection with WNV-E218A.

(F) Survival analysis of mice with oligodendrocyte-specific deletion of IL-33 following intracranial infection of 2e4 PFU WNV-E218A.

(A-E) Data are representative of two independent experiments. (F) Data are representative of 3 pooled independent experiments (error bars, SEM). * $p < 0.05$, ** $p < 0.01$, *** $p < 0.001$. (C and E) two-tailed student's T test (F) (Gehan-Breslow-Wilcoxon test).

bioRxiv preprint doi: https://doi.org/10.1101/2023.04.11.536332; this version posted April 12, 2023. The copyright holder for this preprint (which was not certified by peer review) is the author/funder, who has granted bioRxiv a license to display the preprint in perpetuity. It is made available under aCC-BY 4.0 International license.

Fig 3. IL-33/ST2 signaling on adaptive immune cells does not impact host survival following intracranial flavivirus infection

(A) Cell number and CD44/CD69 gMFI of indicated adaptive immune cell types per ½ brain by FACs 7 days post intracranial infection with WNV-E218A.

(B) Cell number and CD44/CD69 gMFI of indicated adaptive immune cell types per ½ brain by FACs 7 days post intracranial infection with ZIKV-Dakar.

(C) Percent ST2+ and ST2 gMFI of indicated immune cell types 7 days post vehicle injection.

(D) Percent ST2+ and ST2 gMFI of immune cells 7 days post intracranial infection with WNV-E218A.

(E) Survival analysis of mice with Treg deletion of ST2 following intracranial ZIKV-Dakar infection.

Data are representative of 2 pooled independent experiments (error bars, SEM). * $p < 0.05$, ** $p < 0.01$, *** $p < 0.001$ (A, B) (2-way ANOVA with Holm-Sidak Multiple comparisons) (C, D) (One-way ANOVA with Holm-Sidak Multiple comparisons). (E) (Gehan-Breslow-Wilcoxon test)

Fig 4. IL-33/ST2 signaling is necessary for microglial activation and host defense following CNS flavivirus infection.

bioRxiv preprint doi: https://doi.org/10.1101/2023.04.11.536332; this version posted April 12, 2023. The copyright holder for this preprint (which was not certified by peer review) is the author/funder, who has granted bioRxiv a license to display the preprint in perpetuity. It is made available under aCC-BY 4.0 International license.

(A) Representative immunofluorescent images of microglial activation and IL-33 cell loss in hippocampal CA3 with increasing doses of intracranial WNV-E218A (20x magnification, scale bars, 100 microns).

(B) Quantification of IL-33+ cell number, macrophage activation, and their correlation in hippocampal CA3 with increasing doses of intracranial WNV-E218A.

(C) Representative immunofluorescent images of Iba1+ microglia in B6/J and *Il1rl1*$^{-/-}$ mice 7 days post-infection with WNV-E218A (20x magnification, scale bars, 100 microns).

(D) Quantification of Iba1 by MFI in indicated brain regions of B6/J and *Il1rl1*$^{-/-}$ mice 7 days post-infection with WNV-E218A.

(E) Survival analysis of mice with microglial-specific deletion of ST2 following intracranial infection with WNV-E218A.

Data are representative of 2 and 3 (E) pooled independent experiments (error bars, SEM). * $p < 0.05$, ** $p < 0.01$, *** $p < 0.001$. (B, D) (2-way ANOVA with Holm-Sidak Multiple comparisons and Pearson's Correlation) (E) (Gehan-Breslow-Wilcoxon test).

Fig 5. *Il33*$^{-/-}$ hippocampal macrophages exhibit enhanced inflammatory and cell stress responses acutely during CNS WNV infection.

(A) Scheme of hippocampal macrophage isolation and RNAsequencing following intracranial WNV-E218A infection of B6/J and *Il33*$^{-/-}$ mice.

(B) Principal Component Analysis of RNAseq samples.

(C) Volcano plot showing differential gene expression in *Il33*$^{-/-}$ vs. B6/J hippocampal macrophages post-infection.

bioRxiv preprint doi: https://doi.org/10.1101/2023.04.11.536332; this version posted April 12, 2023. The copyright holder for this preprint (which was not certified by peer review) is the author/funder, who has granted bioRxiv a license to display the preprint in perpetuity. It is made available under aCC-BY 4.0 International license.

(D) Top 20 Hallmark gene sets enriched in *Il33*$^{-/-}$ relative to B6/J hippocampal macrophages post-infection.

Fig 6. Disruption of IL-33 signaling during CNS WNV infection induces brain macrophage apoptosis and neuronal pathology.

(A) %ZombieNIR+ dying cell populations of indicated type by FACs analysis of brain homogenates 7 days post-infection with WNV-E218A in B6/J and *Il1rl1*$^{-/-}$ mice.

(B) Representative images of CC3+ CA3 hippocampal brain macrophages 7 days post-infection with WNV-E218A in B6/J and *Il33*$^{-/-}$ mice (20x magnification, scale bars, 100 microns). Arrowheads indicate Iba1-CC3+ while arrows indicate Iba1+CC3+ cells.

(C) Quantification of CC3+ CA3 hippocampal brain macrophages.

(D) Quantification of monocyte count by FACs analysis of brain homogenates in B6/J and *Il1rl1*$^{-/-}$ mice 7 days post WNV-E218A infection.

(E) Representative images of monocyte engraftment in hippocampal CA3 and cerebellum of B6/J and *Il1rl1*$^{-/-}$ mice 7 days post WNV-E218A infection (20x magnification, scale bars, 100 microns). Arrowheads indicate Iba1-CD68+ cells.

(F) Quantification of CD68+Iba1- monocytes in hippocampal CA3 and cerebellum.

(G) Representative images of pCJun+ cells and IgG deposition in hippocampal CA3 7 days post-infection with WNV-E218A in B6/J and *Il33*$^{-/-}$ mice (20x magnification, scale bars, 100 microns). Arrowheads indicated pCJun+ cells.

(H) Quantification of pCJun+ cells and IgG MFI.

bioRxiv preprint doi: https://doi.org/10.1101/2023.04.11.536332; this version posted April 12, 2023. The copyright holder for this preprint (which was not certified by peer review) is the author/funder, who has granted bioRxiv a license to display the preprint in perpetuity. It is made available under aCC-BY 4.0 International license.

(I) Representative images of pCJun+ projections and GFAP+ cells hippocampal CA3 7 days post-infection with WNV-E218A in B6/J and *Il33*$^{-/-}$ mice (20x magnification, scale bars, 100 microns).

(J) Quantification of GFAP+ area and pCJun+ projection area.

(K) Representative images of CC3+ neurons in hippocampal CA3 and cerebellum of B6/J and *Il1rl1*$^{-/-}$ mice 7 days post WNV-E218A infection (20x magnification, scale bars, 100 microns). Arrowheads indicate NeuN+CC3+ cells.

(L) Quantification of CC3+ neuron number in CA3 and cerebellum.

Data are representative of 2 (A-F) independent and 2 (G-N) pooled independent experiments (error bars, SEM). * $p < 0.05$, ** $p < 0.01$, *** $p < 0.001$. (A, C, H) (two-tailed T test) (E, G, J, L) (Two-way ANOVA with Holm-Sidak multiple comparisons).

Supplemental Figures

Fig S1 (related to Fig 1). The IL-33 pathway improves disease outcomes across multiple models of flavivirus infection

(A) Survival analysis of adult B6/J mice exposed to increasing doses of intracranial WNV-E218A and WNV-Tx.

(B) Weight loss of *Il33*$^{-/-}$, *Il1rl1*$^{-/-}$, and B6/J mice following 2e4 PFU WNV-E218A intracranial infection.

(C) Weight loss of *Il33*$^{-/-}$, *Il1rl1*$^{-/-}$, and B6/J mice following 1e6 PFU ZIKV-Dakar intracranial infection.

bioRxiv preprint doi: https://doi.org/10.1101/2023.04.11.536332; this version posted April 12, 2023. The copyright holder for this preprint (which was not certified by peer review) is the author/funder, who has granted bioRxiv a license to display the preprint in perpetuity. It is made available under aCC-BY 4.0 International license.

(D) Survival analysis of *Il1rl1*$^{-/-}$ and B6/J mice following footpad infection with 100 PFU WNV-Tx.

(E) Weight loss of *Il1rl1*$^{-/-}$ and B6/J mice following footpad infection with 100 PFU WNV-Tx.

Data are representative of 3 pooled independent experiments (error bars, SEM). * $p < 0.05$, ** $p < 0.01$, *** $p < 0.001$ (A, D) (Gehan-Breslow-Wilcoxon test) (B, C, E) (2-way ANOVA with Holm-Sidak Multiple comparisons).

Fig S2 (related to Fig 2). Deletion of IL-33 in oligodendrocytes with tamoxifen treatment of *Plp1*$^{ERT2Cre/+}$::*Il33*$^{fl/fl}$ mice

(A) GFAP+ cell number by immunohistochemistry following intracranial infection with increasing doses of WNV-E218A.

(B) Scheme for tamoxifen injections to induce IL-33 excision and representative images of IL-33 loss in cortical oligodendrocytes following tamoxifen treatment (20x magnification, scale bars, 50 microns). Arrowheads Indicate Olig2+IL-33+ cells.

(C) Quantification of total cortical oligodendrocyte number and IL-33+ oligodendrocytes following tamoxifen injection.

Data are representative of 3 pooled independent experiments (error bars, SEM). *** $p < 0.001$. (C) two-tailed student's T test.

Fig S3 (related to Fig 3). ST2 is highly expressed on adaptive immune subsets, but this expression is dispensible for host survival.

(A) Scheme for CD8 T cell depletion during intracranial WNV-E218A infection.

bioRxiv preprint doi: https://doi.org/10.1101/2023.04.11.536332; this version posted April 12, 2023. The copyright holder for this preprint (which was not certified by peer review) is the author/funder, who has granted bioRxiv a license to display the preprint in perpetuity. It is made available under aCC-BY 4.0 International license.

(B) Peripheral blood counts 6 DPI to confirm CD8 depletion.

(C) Survival analysis of mice with CD8 T cell depletion and WNV-E218A intracranial infection.

(D) Weight change in mice with CD8 T cell depletion and control IgG injection following WNV-E218A intracranial infection.

(E) Representative FACs plots and gating strategy for indicated cell types from brain homogenate 7 days post intracranial WNV-E218A infection.

(F) Representative FACs plots of ST2 expression on indicated cell types from B6/J and *Il1rl1*$^{-/-}$ brain homogenate 7 days post intracranial WNV-E218A infection.

(G) Quantification of ST2 excision on splenic and liver Tregs of indicated genotype one-month post tamoxifen treatment.

(H) Weight change in mice with Treg ST2 deletion following intracranial infection with ZIKV-Dakar

(I) Scheme and cell number from peripheral blood of indicated immune cells following IL-2 complex treatment and WNV-E218A infection at 9 DPI.

(J) gMFI of CD25 and GITR on peripheral blood Tregs at 9 DPI with WNV-E218A and IL-2 complex treatment.

(K) Survival analysis of mice with control or IL-2 complex treatment following intracranial infection with WNV-E218A.

(L) Weight change in mice with control or IL-2 complex treatment after intracranial infection with WNV-E218A.

bioRxiv preprint doi: https://doi.org/10.1101/2023.04.11.536332; this version posted April 12, 2023. The copyright holder for this preprint (which was not certified by peer review) is the author/funder, who has granted bioRxiv a license to display the preprint in perpetuity. It is made available under aCC-BY 4.0 International license.

Data are representative of 2 pooled independent experiments (error bars, SEM). * $p < 0.05$, ** $p < 0.01$, *** $p < 0.001$. (B, D, G, J, H, L) (2-way ANOVA with Holm-Sidak Multiple comparisons) (C, K) (Gehan-Breslow-Wilcoxon test) (I) (Student's two-tailed t Test).

Fig S4 (related to Fig 4). Phenotypes of ST2 signaling on microglial activation during CNS Flavivirus infection.

(A) Representative immunofluorescent images of Iba1+ brain macrophages in B6/J and *Il1rl1*$^{-/-}$ mice 7 days post vehicle injection (20x magnification, scale bars, 100 microns).

(B) Quantification of Iba1 gMFI in vehicle injected mice of indicated brain regions.

(C) Representative immunofluorescent images of Iba1+ brain macrophages in B6/J and *Il1rl1*$^{-/-}$ mice 10 days post WNV-E218A infection (20x magnification, scale bars, 100 microns).

(D) Quantification of Iba1 MFI 10 days post WNV-E218A infection in hippocampal CA3 of B6/J and *Il1rl1*$^{-/-}$ mice.

(E) Representative immunofluorescent images of C1q deposition in hippocampal CA3 of B6/J and *Il33*$^{-/-}$ mice 7 days post-infection (20x magnification, scale bars, 100 microns).

(F) Quantification of C1q gMFI by immunofluorescence in hippocampal CA3 of B6/J and *Il33*$^{-/-}$ mice 7 days post-infection.

(G) Representative FACs plots of microglia from CX3CR1$^{ERT2Cre/+::}$ *Il1rl1*$^{fl/fl}$ 30 days post tamoxifen treatment and following CD11b enrichment by MACs.

(H) Quantification of MACs enrichment efficiency.

(I) Quantification of *Il1rl1* signal by qRT-PCR of sorted microglia 30 days post tamoxifen treatment and following CD11b enrichment by MACs.

bioRxiv preprint doi: https://doi.org/10.1101/2023.04.11.536332; this version posted April 12, 2023. The copyright holder for this preprint (which was not certified by peer review) is the author/funder, who has granted bioRxiv a license to display the preprint in perpetuity. It is made available under aCC-BY 4.0 International license.

(J) Weight change in CX3CR1$^{ERT2Cre/+::}$ *Il1rl1*$^{fl/fl}$ mice following intracranial infection of WNV-E218A.

(K) Survival analysis of mice with neuronal *Il1rl1* deletion following intracranial infection with WNV-E218A.

(L) Weight change of mice with neuronal *Il1rl1* deletion following intracranial infection with WNV-E218A.

Data are representative of 2 (A-F) independent and 2 (G-N) pooled independent experiments (error bars, SEM). * $p < 0.05$, ** $p < 0.01$, *** $p < 0.001$. (B, F, H, L) (two-tailed T test) (D, I, J, N) (Two-way ANOVA with Holm-Sidak multiple comparisons) (M) (Gehan-Breslow-Wilcoxon test).

Fig S5 (related to Fig 5). Hallmark pathways enriched in *Il33*$^{-/-}$ hippocampal macrophages during WNV infection.

(A) Volcano plot showing enriched genes in *Il33*$^{-/-}$ hippocampal macrophages relative to B6/J with vehicle injection.

(B) Top 20 significantly enriched Hallmark gene sets by GSEA of *Il33*$^{-/-}$ and B6/J hippocampal macrophages post-infection in vehicle-injected samples.

(C) Heatmap of Inflammatory Response pathway genes in indicated samples.

(D) Heatmap of Fatty Acid Metabolism pathway genes in indicated samples.

(E) Heatmap of Oxidative Phosphorylation pathway genes in indicated samples.

(F) Heatmap of Hypoxia pathway genes in indicated samples.

(G) Heatmap of Apoptosis pathway genes in indicated samples.

bioRxiv preprint doi: https://doi.org/10.1101/2023.04.11.536332; this version posted April 12, 2023. The copyright holder for this preprint (which was not certified by peer review) is the author/funder, who has granted bioRxiv a license to display the preprint in perpetuity. It is made available under aCC-BY 4.0 International license.

Fig S6 (related to Fig 6) IL-33 signaling prevents brain macrophage apoptosis following intracranial ZIKV-Dakar infection.

(A) Representative images of CC3+ hippocampal CA1 brain macrophages in B6/J and *Il33*$^{-/-}$ mice 7 days post-infection with WNV-E218A (20x magnification, scale bars, 100 microns).

(B) Quantification of CC3+ hippocampal CA1 brain macrophages in B6/J and *Il33*$^{-/-}$ mice.

bioRxiv preprint doi: https://doi.org/10.1101/2023.04.11.536332; this version posted April 12, 2023. The copyright holder for this preprint (which was not certified by peer review) is the author/funder, who has granted bioRxiv a license to display the preprint in perpetuity. It is made available under aCC-BY 4.0 International license.

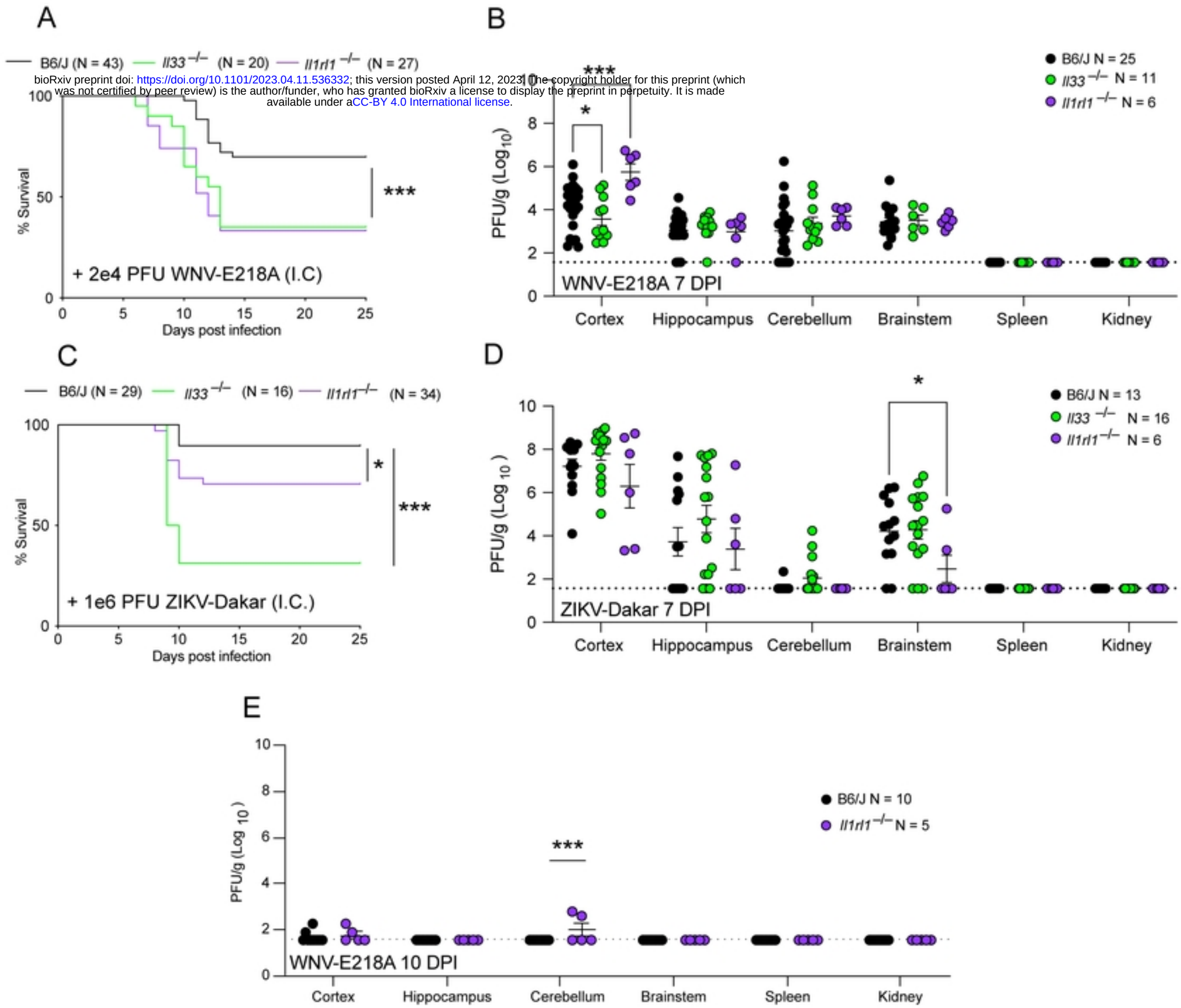

Figure 1. The IL-33 pathway promotes survival upon neuroinvasive flavivirus infection, independent of viral control

Figure 1

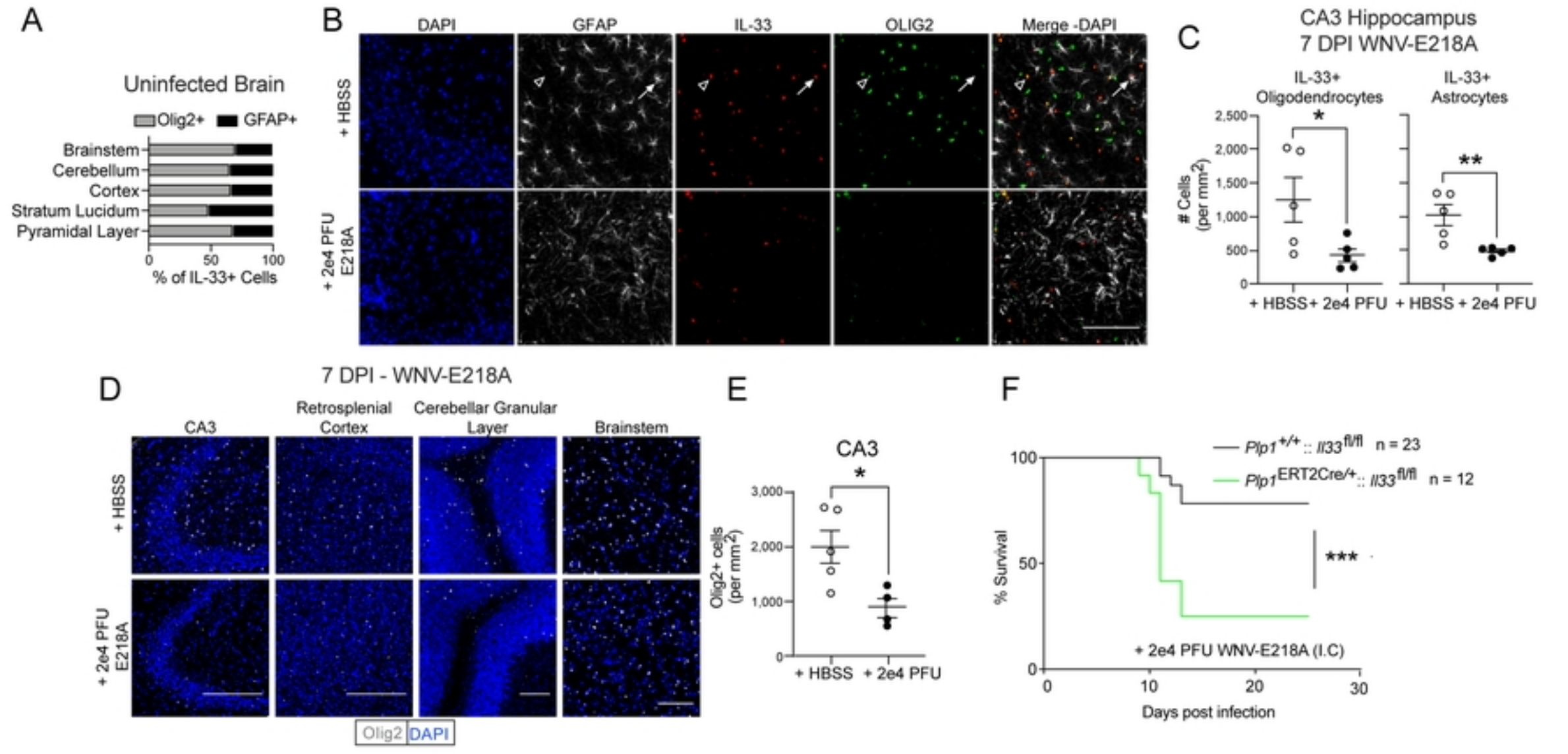

Figure 2. Oligodendrocyte-derived IL-33 promotes survival to neurotropic flavivirus infection

Figure 2

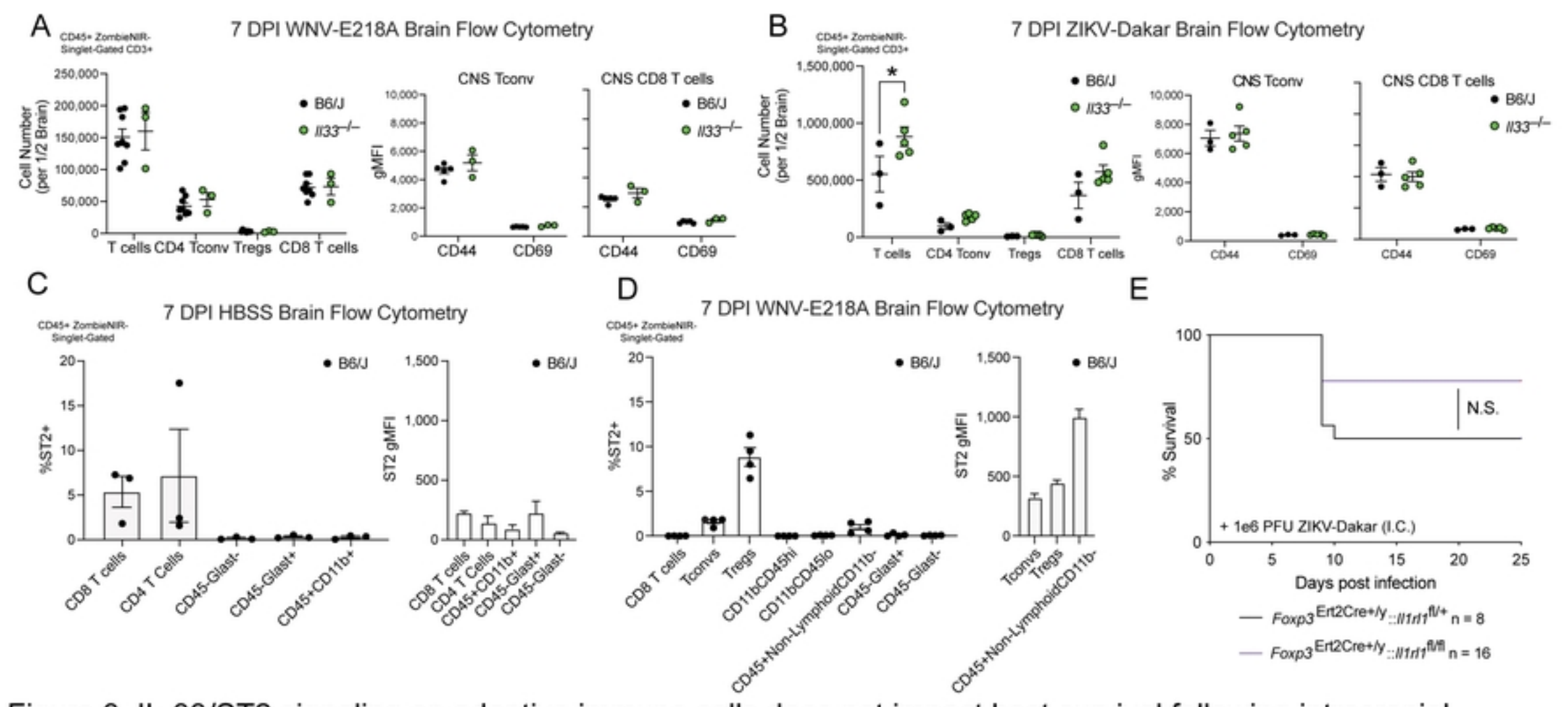

Figure 3. IL-33/ST2 signaling on adaptive immune cells does not impact host survival following intracranial flavivirus infection

Figure 3

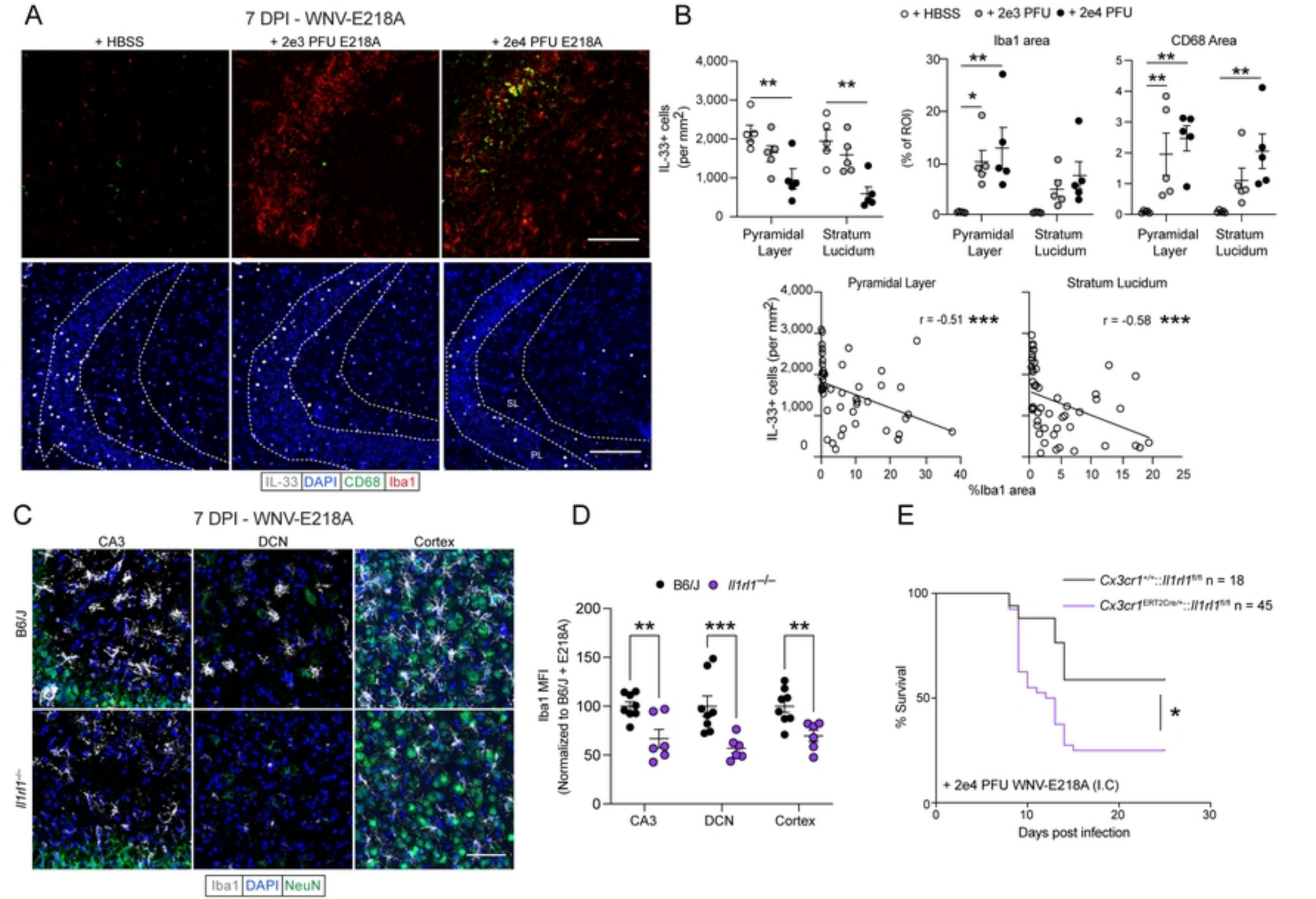

Figure 4. IL-33/ST2 signaling is necessary for microglial activation and host defense following CNS flavivirus infection.

Figure 4

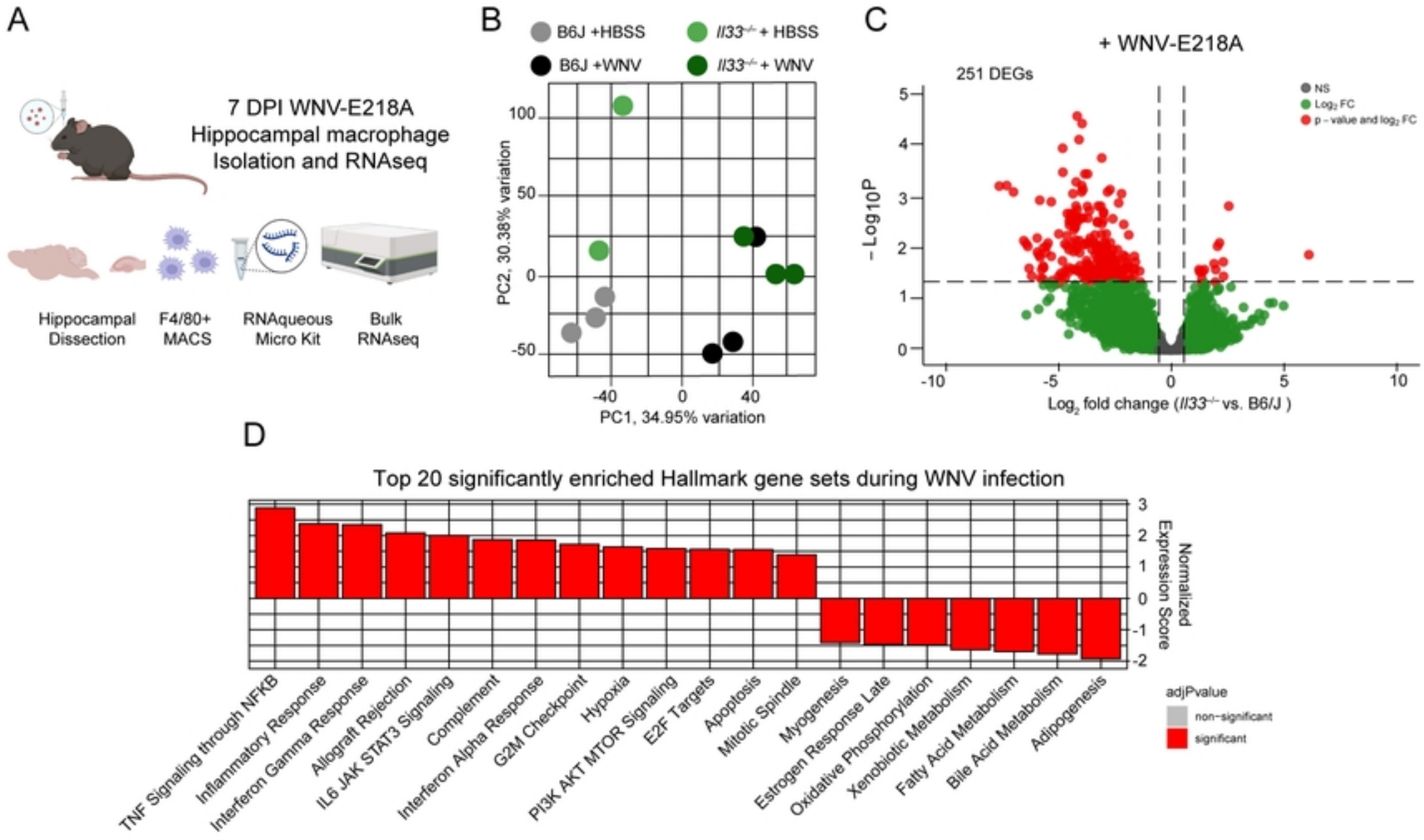

Figure 5. *Il33*$^{-/-}$ Hippocampal macrophages exhibit enhanced inflammatory and cell stress responses acutely during CNS WNV infection.

Figure 5

bioRxiv preprint doi: https://doi.org/10.1101/2023.04.11.536332; this version posted April 12, 2023. The copyright holder was not certified by peer review) is the author/funder, who has granted bioRxiv a license to display the preprint in perpetuity. It is made available under aCC-BY 4.0 International license.

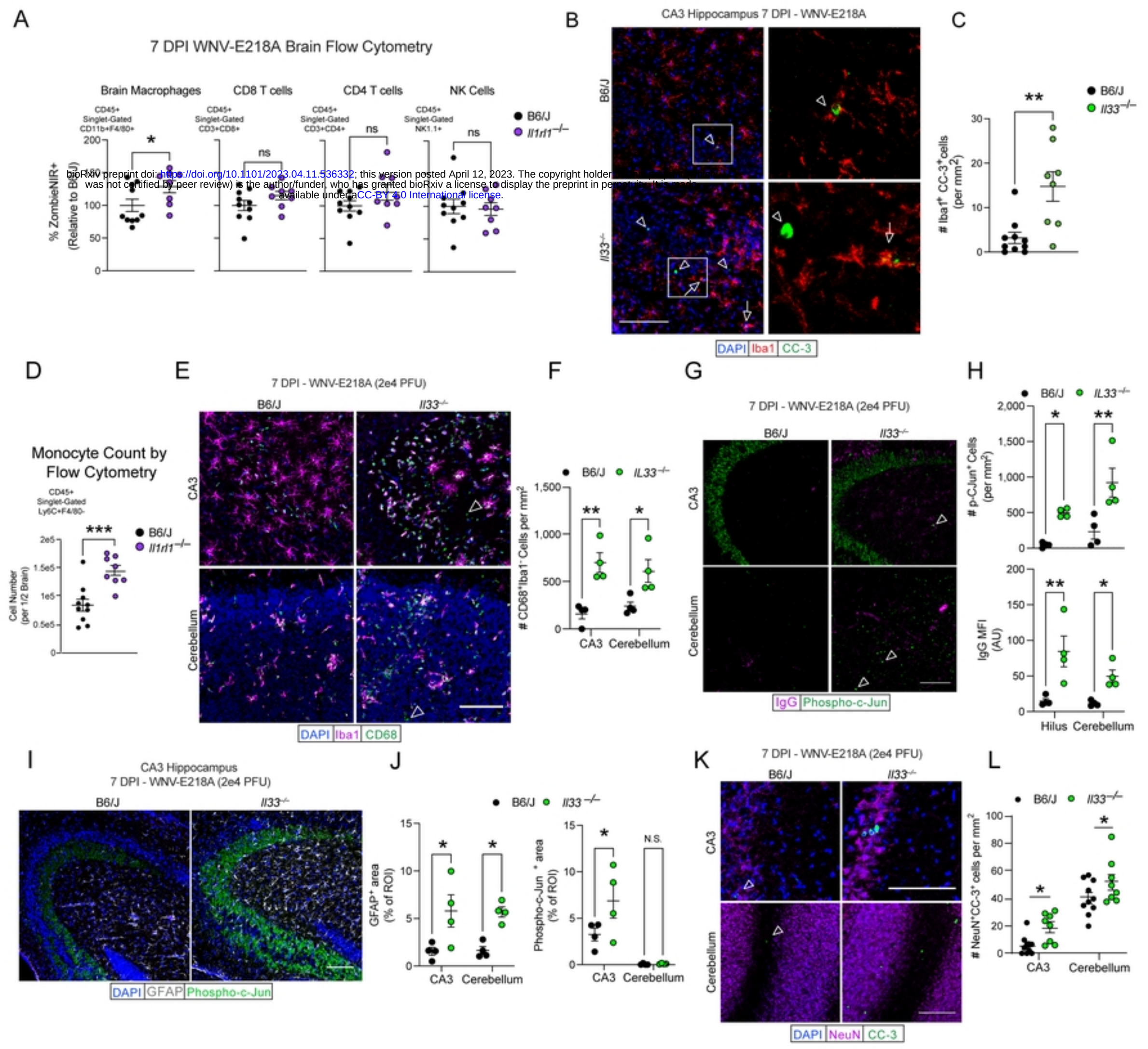

Figure 6. Disruption of IL-33 signaling during CNS WNV infection induces brain macrophage apoptosis and neuronal pathology.

Figure 6